Transformations in the Transition Metal Carbonyls Containing Arsenic: Exploring the Chemistry of $[Et_4N]_2[HAs\{Fe(CO)_4\}_3]$ in the Search for Single Source Precursors for Advanced Metal Pnictide Materials

Desmond E. Schipper, Benjamin E. Young, and Kenton H. Whitmire*

Department of Chemistry, MS60
Rice University 6100 Main Street
Houston, TX 77005
Supporting Information Placeholder

ABSTRACT: The chemistry of $[Et_4N]_2[HAs\{Fe(CO)_4\}_3]$ ($[Et_4N]_2[\mathbf{I}]$) has been explored with the goal of preparing heterometallic compounds for use as single source precursors to metal pnictide phases. Reaction of $AgPF_6$ with $[Et_4N]_2[\mathbf{I}]$ in THF produces $[Et_4N][HAs\{Fe_2(CO)_6(\mu\text{-}CO)(\mu\text{-}H)\}\{Fe(CO)_4\}]$ in 12% yield, but the yield is improved to 71% if the reaction is carried out with added $[Et_4N][HFe(CO)_4]$. The structure possesses rare As-H and $\{Fe_2(CO)_6(\mu\text{-}CO)(\mu\text{-}H)\}$ fragments. The addition of $[CPh_3][BF_4]$ to $[Et_4N]_2[\mathbf{I}]$ in THF yields $[Et_4N][Fe_3(CO)_9(\mu\text{-}CO)\{\mu_3\text{-}AsFe(CO)_4\}]$ in 45% yield. This compound is also obtained as a minor product from oxidation of $[Et_4N]_2[\mathbf{I}]$ with one equivalent of $AgPF_6$, $AsCl_3$, $SbCl_3$, or $BiCl_3$ in THF. The cluster consists of an Fe_3As tetrahedron with an isolated $Fe(CO)_4$ unit bound to the arsenic in a spiked tetrahedral arrangement. Refluxing $[Et_4N]_2[\mathbf{I}]$ with one equivalent of $AgPF_6$ in THF produces $[Et_4N][(\mu\text{-}H)_2Fe_3(CO)_9\{\mu_3\text{-}AsFe(CO)_4\}]$. This cluster is similar to $[Et_4N][Fe_3(CO)_9(\mu\text{-}CO)\{\mu_3\text{-}AsFe(CO)_4\}]$ with the bridging CO being replaced by two bridging hydride ligands. Treatment of $[Et_4N]_2[\mathbf{I}]$ with one equivalent of $Mn(CO)_5Br$ in THF yields the spirocyclic compound $[Et_4N][\{FeMn(CO)_8\}(\mu_4\text{-}As)\{Fe_2(CO)_6(\mu\text{-}CO)(\mu\text{-}H)\}]$ in 52% yield. Refluxing this cluster in the presence of triethylamine and an additional 1.8 equivalents of $Mn(CO)_5Br$ yields $[Et_4N][Fe_3(CO)_9(\mu\text{-}CO)\{\mu_3\text{-}AsMn(CO)_4Br\text{-}cis\}]$ in low yield. Alternatively, treating $[Et_4N][\{FeMn(CO)_8\}(\mu_4\text{-}As)\{Fe_2(CO)_6(\mu\text{-}CO)(\mu\text{-}H)\}]$ with triflic acid or an oxidant ([Ox] = Cu^+, Ag^+, Cu^{2+}, or CPh_3^+) in dichloromethane produces the two neutral compounds $(\mu\text{-}H)_2Fe_3(CO)_9\{\mu_3\text{-}AsMn(CO)_5\}$ and $\{FeMn(CO)_8\}(\mu_4\text{-}As)\{Fe_2(CO)_8\}$ in trace amounts and high yield, respectively. The former could be removed by treatment with base in nonpolar solvents. Neutral $\{FeMn(CO)_8\}(\mu_4\text{-}As)\{Fe_2(CO)_8\}$can then be isolated by filtration and evaporation in 74% yield. An improved synthesis of the known $[Fe_3(CO)_9(\mu\text{-}CO)\{\mu_3\text{-}PFe(CO)_4\}]^-$ as its tetraethylammonium salt is also included. All compounds were characterized spectroscopically, by ESI-Mass Spectrometry, and by single crystal X-ray diffraction.

INTRODUCTION

A major thrust of research in our laboratory has been the development of single-source precursors (SSPs) for complex binary and ternary metal pnictides, systems in which multiple phases are possible for a given combination of elements. In contrast to systems like those of cadmium sulfide and cadmium selenide where only one phase for the combination of elements exists, iron phosphide has multiple combinatory mixtures possible: FeP_4, FeP_2, FeP, Fe_2P, and Fe_3P, each with discrete phases and structures.[1] These compositional and structural differences create a diverse and attractive set of properties unique to each combinatory mixture. For example, FeP_2 and FeP have been demonstrated to exhibit superior anode performance for Li^+ ion batteries,[2–4] FeP ultra-high performance as the hydrogen evolution cathode in water-splitting catalysis,[5–8] and Fe_2P high activity as a hydrodesulfurization and hydrodenitrogenation catalyst.[9,10] Moreover, Fe_3P is known for its high Curie temperature of 716 K and ability to catalyze carbon nanotube growth.[11,12]

Conventional methods of preparing thin films and nanoparticles of metal phosphides often require harsh conditions with limited phase control.[13–22] Our work with SSPs and that of others has shown that specific phases of the metal pnictide family can be targeted successfully. For example, we demonstrated that the precursor $H_2Fe_3(CO)_9P^tBu$ would yield thin films of Fe_3P by MOCVD at 400 °C and that $FeMn(CO)_8(\mu\text{-}PH_2)$ could be converted into the high-temperature hexagonal phase of FeMnP at 350 °C by bulk pyrolysis as well as in solvents to yield nanoparticles of $Fe_{2-x}Mn_xP$.[23–25] Scheer et al. have demonstrated that $Fe(CO)_4PH_3$ and $[(CO)_4Cr(\mu\text{-}PH_2)]_2$ can be converted to nanoparticles of FeP or CrP under mild conditions.[26,27] In each instance, the metal ratio contained in the precursor was conserved, although in the case of FeMnP some leaching of the Mn was observed if oleic acid was present in the surfactant mixture. The success of these precursors in achieving their target materials can largely be attributed to the intimate mixing of the heavy elements achieved upon decomposition due to the unimolecular nature of the precursor, the pre-determined stoichiometry built into the molecule, the chemical inertness of the carbonyl ligand environment, and the relative weakness of the P-H bonds.

Recently, we have turned our attention to syntheses of precursors for the system $Fe_{2-x}Mn_xAs_{1-y}P_y$, a quaternary metal pnictide possessing a giant magnetocaloric effect at near-ambient temperature.[28] Such an endeavor is synthetically challenging as an ideal SSP would require a single molecule to contain two iron atoms, two manganese atoms, one phosphorus atom, and one arsenic atom. An alternative strategy is to co-decompose precursors that are isostructural, e.g. $FeMn(CO)_8(\mu\text{-}PH_2)$ and $FeMn(CO)_8(\mu\text{-}AsH_2)$. The latter strategy would allow for a wider range of compositional variation. Additionally, it would be advantageous to have high yield, clean routes that avoid the use of toxic, volatile organoarsines. This investigation led us to explore the use of $[Et_4N]_2[HAs\{Fe(CO)_4\}_3]$ ($[Et_4N]_2$[**I**]), an easily prepared cluster containing iron and arsenic as a starting material.[29] There are few clusters containing Fe, Mn and As, and none which can be prepared in high yield or with only a carbonyl or carbonyl/hydride ligand environment.[30–36] Previous work has shown that protonation of $[Et_4N]_2$[**I**] gives $As_2Fe_6(CO)_{22}$ (**II, Scheme 1**) while pyrolysis yielded $[Et_4N][Fe_3(CO)_9\{\mu_3\text{-}AsFe(CO)_4\}_2]$ ($[Et_4N]_2$[**III**]).[37] Neither of these clusters has the desired stoichiometry for known Fe-As phases but may be useful for preparation of higher order materials containing P or another transition metal.

Scheme 1. Known Transformations of $[Et_4N]_2$[**I**]

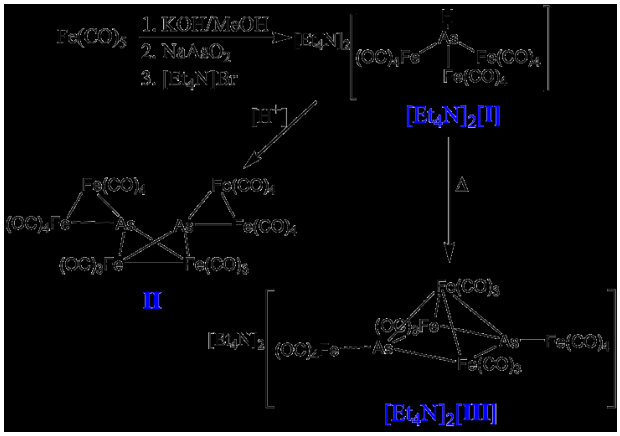

In efforts to develop this chemistry further, we have examined the fundamental chemistry of $[Et_4N]_2$[**I**] with oxidation and nucleophilic displacement as synthetic strategies. Herein, we report the synthesis and isolation of the new Fe-As carbonyl clusters $[Et_4N][HAs\{Fe_2(CO)_6(\mu\text{-}CO)(\mu\text{-}H)\}\{Fe(CO)_4\}]$ ($[Et_4N]$[**IV**]), $[Et_4N][Fe_3(CO)_9(\mu\text{-}CO)(\mu_3\text{-}AsFe(CO)_4]$ ($[Et_4N]_2$[**V**]), and $[Et_4N][(\mu\text{-}H)_2Fe_3(CO)_9(\mu_3\text{-}AsFe(CO)_4]$ ($[Et_4N]$ [**VI**]). Applying the same sort of considerations to the introduction of manganese, we obtained $[Et_4N][\{FeMn(CO)_8\}(\mu_4\text{-}As)\{Fe_2(CO)_6(\mu\text{-}CO)(\mu\text{-}H)\}]$ ($[Et_4N]$[**VII**]) in high yield. This compound further reacts to produce $[Et_4N][\{Fe_3(CO)_9(\mu\text{-}CO)\}(\mu_4\text{-}As)\{cis\text{-}Mn(CO)_4Br\}]$ ($[Et_4N]$[**VIII**]) and $(\mu\text{-}H)_2Fe_3(CO)_9\{\mu_3\text{-}AsMn(CO)_5\}$ (**IX**) in low yield and $\{FeMn(CO)_8\}(\mu_4\text{-}As)\{Fe_2(CO)_8\}$ (**X**) in high yield. These studies provide insight into the chemistry of arsenic in metal carbonyl clusters and the reactivity of an arsenic-bound hydride.

RESULTS AND DISCUSSION

The compound $[Et_4N]_2$[**I**] offers many advantages as a starting material for the synthesis of iron and heterobimetallic clusters containing arsenic. It is a high yield product from simple, inexpensive starting materials. Reduction of sodium arsenite in methanolic KOH by $[HFe(CO)_4]^-$ yields $[\mathbf{I}]^{2-}$ which can be precipitated by addition of $[Et_4N]Br$. In this form, it is stable indefinitely under an inert atmosphere. This route to introducing arsenic into metal carbonyl clusters avoids the use of the toxic and volatile AsH_3 or organoarsines. Synthetic strategies can take advantage of the dianionic nature of $[\mathbf{I}]^{2-}$ and/or its reactive arsenic-bound hydride. Metathesis reactions with cationic metal centers could result in the addition of metal fragments, but its high electron charge also gives $[\mathbf{I}]^{2-}$ reducing power - it can reduce Cu^{2+} to Cu^0 readily, for example. This opens up multiple potential strategies for using $[\mathbf{I}]^{2-}$ to produce Mn-Fe-As Compounds. One strategy is deprotonation to create a highly reactive trianion that is likely to only be stable at low temperatures. Alternatively, the hydride can be abstracted with a hydride-abstraction agent to yield an unsaturated and electrophilic $[As\{Fe(CO)_4\}_3]^-$ intermediate. The hydride could also be homolytically cleaved to yield an anionic radical species $[^{\bullet}As\{Fe(CO)_4\}_3]^{2-}$.

In this study, we have evaluated the effects of oxidation and hydrogen abstraction for $[\mathbf{I}]^{2-}$ as well as various routes for adding an $Mn(CO)_x$ fragment to the cluster. The first part of the discussion will describe the iron only compounds, and the second part will focus on addition of Mn to $[\mathbf{I}]^{2-}$ to form $[\mathbf{VII}]^-$ and its subsequent transformation to $[\mathbf{VIII}]^-$, **IX**, and **X**.

Synthesis and Reactivity of Fe/As Compounds

Compound $[Et_4N]_2$[**I**] reacts with either Ag^+ or Cu^+ to yield the new Fe-As carbonyl cluster anions $[\mathbf{IV}]^-$, $[\mathbf{V}]^-$, and $[\mathbf{VI}]^-$. $[Et_4N][\mathbf{IV}]$ was first obtained in low yield from the reaction of a one-electron oxidant (Ox = Ag^+, Cu^+) with $[Et_4N]_2$[**I**] (**Equation 1**). While the reaction appears to be initiated by an oxidation process, $[\mathbf{IV}]^-$ is not formally an oxidation product. One could envision formation of $[\mathbf{IV}]^-$ to arise via a simple CO loss process that would result in the formation of an Fe-Fe bond with subsequent protonation of that bond. The metal-metal bond formation reaction upon loss of CO is well-documented. For example, the chalcogenide analogs of $[\mathbf{I}]^{2-}$, $[E\{Fe(CO)_4\}_3]^{2-}$ and (E = Se, Te), convert in the absence of a CO atmosphere to tetrahedral $[EFe_3(CO)_9]^{2-}$.[38] The resulting hypothetical intermediate in this case would be $[HAs\{Fe(CO)_4\}\{Fe_2(CO)_6(\mu\text{-}CO)\}]^{2-}$ that would then undergo protonation to produce $[\mathbf{IV}]^-$. But, such closure has not been observed for $[\mathbf{I}]^{2-}$, and simple protonation of $[\mathbf{I}]^{2-}$ in methanol with aqueous HCl gives **II** instead (**Scheme 1**). If the oxidation reaction is performed with added $[HFe(CO)_4]^-$ the product distribution was radically changed. In this case, $[\mathbf{IV}]^-$ was the majority product, $[\mathbf{III}]^{2-}$ was not detected, whereas a small amount of $[Fe_2(CO)_8]^{2-}$ could be seen by FTIR (**Equation 2**).

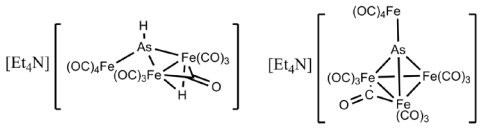

$[Et_4N][\mathbf{IV}]$ $[Et_4N][\mathbf{V}]$

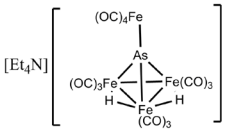

$[Et_4N][\mathbf{VI}]$

(1)

$$[Et_4N]_2[\mathbf{I}] \xrightarrow[\text{2 eq. } [Et_4N][HFe(CO)_4]\text{, THF, RT, 1 h}]{\text{2 eq. } AgPF_6\text{, dropwise add'n}} [Et_4N][\mathbf{IV}] + [Et_4N]_2[Fe_2(CO)_8] \quad (2)$$

71%‡ Detected by IR

A possible mechanism for the formation of $[\mathbf{IV}]^-$ would be the homolytic cleavage of the As-H bond to produce an open $[^{\bullet}As\{Fe(CO)_4\}_3]^{2-}$ radical dianion which could undergo Fe-Fe bond formation to give $[^{\bullet}As\{Fe(CO)_4\}[Fe_2(CO)_6(\mu\text{-}CO)]^{2-}$ with concomitant CO loss (**Scheme 2**). If this species is oxidized, it could combine with another molecule of $[\mathbf{I}]^{2-}$ or with itself to give $[\mathbf{III}]^{2-}$. The formation of $[\mathbf{III}]^{2-}$ could expel an $[HFe(CO)_4]^-$ anion that could then serve as a hydride source from which $[^{\bullet}As\{Fe(CO)_4\}[Fe_2(CO)_6(\mu\text{-}CO)]^{2-}$ could abstract an $H^{\bullet}$ to yield $[HAs\{Fe(CO)_4\}[Fe_2(CO)_6(\mu\text{-}CO)]^{2-}$. Subsequent protonation of this species would yield $[\mathbf{IV}]^-$. This would imply formation of $[^{\bullet}Fe(CO)_4]^-$ which would explain the observation of $[Fe_2(CO)_8]^{2-}$ in the final product distribution. This is consistent with the observation that addition of $[HFe(CO)_4]^-$ greatly improves the yield of $[\mathbf{IV}]^-$ and with the detection of $[Fe_2(CO)_8]^{2-}$ in the final products. If this reaction can be demonstrated with other systems, the treatment of a given "open" cluster with $[HFe(CO)_4]^-$ and a one-electron oxidant might serve as a general route to metal-metal bond formation and introduction of a hydride to a given cluster.

Scheme 2. Possible Reaction Pathways of $[\mathbf{I}]^{2-}$

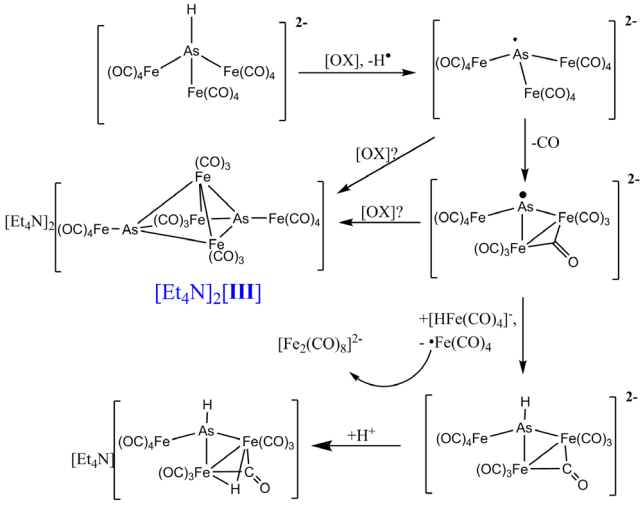

Compound $[Et_4N][\mathbf{V}]$ was obtained from a variety of reactions involving $[\mathbf{I}]^{2-}$ and was isolated as the first product to crystallize out of the ethereal extracts of those reactions. The highest yield (45%) is obtained by treating $[\mathbf{I}]^{2-}$ with the well-known hydride abstraction agent $[CPh_3][BF_4]$ in DCM. Full conversion of $[\mathbf{I}]^{2-}$ to a 1:1 mixture of $[\mathbf{V}]^-$ and $[\mathbf{III}]^-$ is achieved essentially immediately (**Equation 3**). Removal of the solvent after 1 hour, treatment of the solids with diethyl ether, filtration, and storage at -10 ° C yields black plate-like crystals of $[Et_4N][\mathbf{V}]$ overnight. The compound is poorly soluble in ether but will crystallize readily from ethereal solutions. It was obtained in higher yield from treatment of $[\mathbf{I}]^{2-}$ with $AsCl_3$ (35%, **Equation 4**), but use of ECl_3 (E = Sb, Bi) gave only traces. Since pnictogen-halide bonds are known to react with pnictogen-hydride bonds with concomitant HCl evolution in the prototypical "aminolysis-type" reaction,[39] one might postulate that $AsCl_3$ initially reacts with $[\mathbf{I}]^{2-}$ to form an unstable $[Cl_xAs\text{-}As\{Fe(CO)_4\}_3\}_{3-x}]^-$ species which undergoes fragmentation and recombination to yield $[\mathbf{V}]^-$, possibly involving a radical mechanism. Ligand exchange mechanisms between pnictogens are also known.[39] The reaction mechanism is postulated to involve initial hydride abstraction by $[CPh_3]^+$ to yield an unsaturated $[As\{Fe(CO)_4\}_3\}]^-$ species. Such a species could abstract an $Fe(CO)_4$ group from unreacted $[\mathbf{I}]^{2-}$ to yield a sterically crowded $[As\{Fe(CO)_4\}_4]^-$ which would then lose CO to yield $[\mathbf{V}]^-$ as illustrated in **Scheme 3**. The other fragment generated by As-$Fe(CO)_4$ bond scission would interact with a third molecule of $[\mathbf{I}]^{2-}$ to yield $[\mathbf{III}]^{2-}$. Anion $[\mathbf{V}]^-$ is isostructural to the analogous P and Sb compounds $[Fe_3(CO)_9(\mu\text{-}CO)(\mu_3\text{-}EFe(CO)_4]^-$ (E = P, Sb) that have been previously reported.[40,41] A comparison of the three analogs are given in Figure SF3 in the SI. Both the phosphorus and antimony analogs are obtained by treatment of $[Fe_4(CO)_{13}]^{2-}$ with ECl_3 in DCM, a synthesis which bears some similarities to the treatment of $[\mathbf{I}]^{2-}$ with $AsCl_3$ in DCM.

$$[Et_4N]_2[\mathbf{I}] \xrightarrow[CH_2Cl_2\text{, RT, 1 h}]{\text{1 eq. } [CPh_3][BF_4]\text{, dropwise add'n}} [Et_4N]_2[\mathbf{III}] + [Et_4N][\mathbf{V}] \quad (3)$$

~50%* 45%‡

*Yield indicated by IR
‡ Isolated Yield

$$[Et_4N]_2[\mathbf{I}] \xrightarrow[\text{THF, RT, 1 h}]{\text{3.1 eq. } Et_3N\text{, 1 eq. } AsCl_3\text{, dropwise add'n}} [Et_4N][\mathbf{V}] \quad (4)$$

35%*

*Yield indicated by IR

Scheme 3. Proposed mechanism of formation of $[\mathbf{V}]^-$

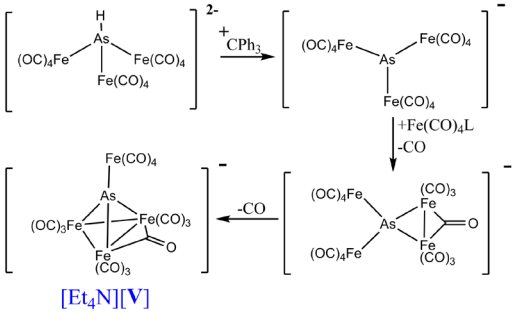

Anion $[\mathbf{VI}]^-$ is isoelectronic and structurally similar to $[\mathbf{V}]^-$; however, the triiron moiety possesses two hydride ligands instead of the bridging carbonyl. Its formation upon reflux of the THF solution from the treatment of $[\mathbf{I}]^{2-}$ with one equivalent of $AgPF_6$ was largely unexpected (**Equation 5**). One might postulate reduction of $[\mathbf{V}]^-$ could promote elimination of CO followed by protonation, similar to the report for the related cluster $[Et_4N][(\mu\text{-}H)_2Fe_3(CO)_9\{\mu_3\text{-}PFe(CO)_4\}]$ by Grossi et al,[42] although our conditions were much milder. Alternatively, $[\mathbf{V}]^-$ could have undergone exchange of its bridging carbonyl with hydrogen generated in the oxidation step to yield the isoelectronic $[\mathbf{VI}]^-$. Attempts to further improve the synthesis of $[\mathbf{VI}]^-$ were not undertaken.

$$[Et_4N]_2[\mathbf{I}] \xrightarrow[\text{THF, }\Delta\text{, 1 h}]{\text{1 eq. } AgPF_6\text{, dropwise add'n}} [Et_4N]_2[\mathbf{III}] + [Et_4N][\mathbf{VI}] \quad (5)$$

~80%* Trace*

*Yield indicated by IR

Synthesis and Reactivity of Fe/Mn/As Compounds

Three sources of manganese were evaluated for their reactivity with $[\mathbf{I}]^{2-}$: $[Et_4N][Mn(CO)_5]$, $Mn_2(CO)_{10}$ and $Mn(CO)_5Br$. Out of these, only $Mn(CO)_5Br$ reacted with $[\mathbf{I}]^{2-}$, although conditions harsher than reflux and UV-irradiation were not explored. $[Et_4N][\mathbf{VII}]$ is obtained upon treatment of $[Et_4N]_2[\mathbf{I}]$ with one equivalent of $Mn(CO)_5Br$ in THF (**Equation 6**).

$$[Et_4N]_2[\mathbf{I}] + Mn(CO)_5Br \xrightarrow{\text{THF, 24 h, RT}} [Et_4N][\mathbf{VII}] \quad (6)$$

52%‡

‡ Isolated Yield (based on As)

After removing the THF, the product was taken up into minimal ether and then stored at -10°C to yield large, red-black single crystals within three days. FT-IR of the solution in the carbonyl stretching region following reaction showed clean conversion to $[\mathbf{VII}]^-$. Hypothetically, electron transfer from $[\mathbf{I}]^{2-}$ to $Mn(CO)_5Br$ replaces the hydride with an $Mn(CO)_5$ fragment and expels HBr as shown in **Scheme 4.** The resulting partially open cluster can close with the hydride either *trans* or *cis* to the $Mn(CO)_4$ fragment. Protonation, ostensibly by byproduct HBr, would yield $[\mathbf{VII}]^-$ as a mixture of the two isomers. $[Et_4N][\mathbf{VII}]^-$ is highly reactive and can be converted to $[\mathbf{VIII}]^-$, **IX** or **X** (**Scheme 5**).

Scheme 4. Possible Mechanism of Formation of $[\mathbf{VII}]^-$

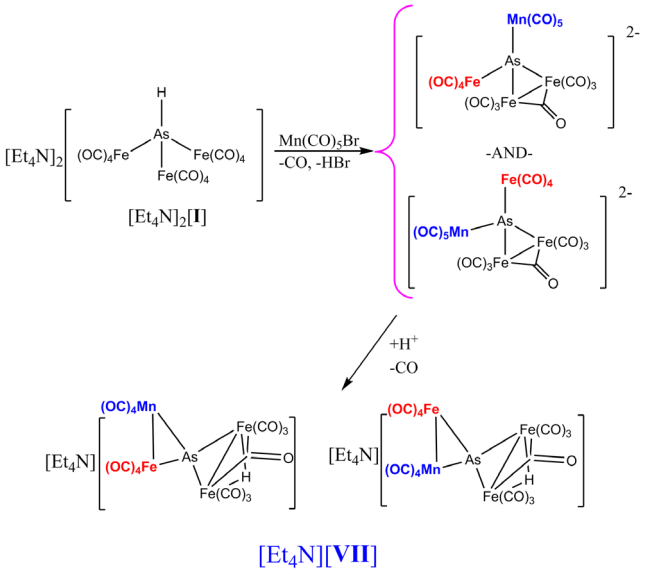

Scheme 5. Synthesis of $[\mathbf{VIII}]^-$, **IX**, and **X**

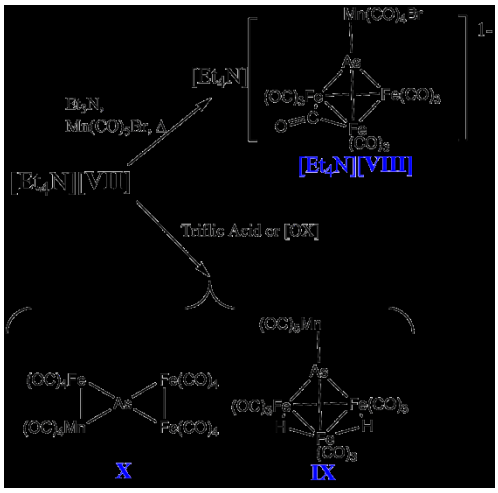

Compound $[\mathbf{VIII}]^-$ forms upon reflux of a solution of $[Et_4N][\mathbf{VII}]$, excess triethylamine, and 1.8 eq. $Mn(CO)_5Br$ (**Equation 7**).

$$[Et_4N]_2[\mathbf{I}] \xrightarrow[\text{2.3.1 eq } Et_3N,\ \text{1.8 eq } Mn(CO)_5Br,\ \Delta\ 3h]{\text{1. 1.0 eq. } Mn(CO)_5Br,\ \text{THF, 24 h}} [Et_4N][\mathbf{VIII}] \quad (7)$$

Trace

Following base addition, the IR stretches for $[\mathbf{VII}]^-$ disappear and $[Mn(CO)_5]^-$ appears in the FTIR spectrum. This suggests $[\mathbf{VII}]^-$ is unstable in the presence of base and eliminates $[Mn(CO)_5]^-$. The resulting cluster could be the $\{Fe_3As(CO)_{10}\}^-$ tetrahedron with a lone pair on the arsenic atom. Such a species could displace CO on $Mn(CO)_5Br$ to produce $[\mathbf{VIII}]^-$, which can be considered an $Mn(CO)_4$(*cis*-Br)L complex.[43]

Anion $[\mathbf{VIII}]^-$ appears after the second portion of $Mn(CO)_5Br$ has been added and the solution refluxed, presumably driving the CO displacement process. Additionally, both the anion $[\mathbf{VIII}]^-$ and an additional species are observed in the ESI mass spectrum at m/z = 768.5 and 884.5. The extra species is consistent with the formula $[Fe_3Mn_2AsC_{19}O_{19}H_{20}N]^-$ and shows CO-loss products (See **SI**). A preliminary but poor data set indicated the composition $[Fe_3(CO)_9(\mu\text{-}CO)\{\mu_3\text{-}AsMn_2(CO)_9\}]^-$ which could be anticipated to form as a product of $[\mathbf{VIII}]^-$ reacting with $Mn(CO)_5Br$ with displacement of bromine. This anion was also observed in the ESI-MS of the reaction solution.

The anion $[\mathbf{VII}]^-$ also serves as a convenient starting point for accessing **IX**, and **X** upon treatment with oxidants (Ox = Ag^+, Cu^+, Cu^{2+}, and CPh_3^+) or triflic acid in DCM. In the case of the oxidants, electron removal could yield an electron deficient cluster which abstracts a CO from another molecule. In the case of the treatment by triflic acid, protonation could occur at the $\{Fe_2(CO)_7H\}$ moiety with H_2 elimination forming an electron-deficient species that abstracts of a CO from another molecule to yield **X**. Compound **X** is produced in high yield along with traces of **IX**, which can be conveniently removed by treatment of the toluene extract of the crude product with triethylamine. The reaction with oxidants takes place immediately, while the conversion with triflic acid takes 24 h (**Equation 8**). The existence of each species was confirmed by ESI-MS (See SI).

$$[Et_4N]_2[\mathbf{I}] \xrightarrow[\text{2. 1.3 eq. Triflic Acid, DCM, 24 h}]{\text{1. 1 eq. } Mn(CO)_5Br,\ RT\ ,\ 24\ h} \mathbf{IX} + \mathbf{X}$$

Trace* 71%‡

*Yield indicated by IR

‡ Isolated Yield (8)

During the course of these studies, many attempts were made to reproduce the synthesis of the $[Fe_3(CO)_9(\mu\text{-}CO)\{\mu_3\text{-}PFe(CO)_4\}]^-$ anion as its tetraphenylphosphonium (Ph_4P^+) or bis(triphenylphosphine)iminium (PPN^+) salt as described in the literature but without success.[40] The IR spectral data given in that report surprisingly did not match the spectra of $[Fe_3(CO)_9(\mu\text{-}CO)\{\mu_3\text{-}EFe(CO)_4\}]^-$ (E = As, Sb) even though the infrared spectra of the As and Sb analogues were nearly identical.[41] The method given for the Sb analog was very similar to the method given for P except for the use of the $[Et_4N]^+$ salts instead of $[PPh_4]^+$ or $[PPN]^+$. Reaction of $[Et_4N]_2[Fe_4(CO)_{13}]$ with PCl_3 yielded $[Fe_3(CO)_9(\mu\text{-}CO)\{\mu_3\text{-}PFe(CO)_4\}]^-$ in 80% yield based on phosphorus (**Equation 9**). The infrared data of the compound prepared in this way matches the As and Sb analogues. ESI-MS of the pure product confirms the cluster's formation with the parent $[Fe_4P(CO)_{14}]^-$ anion observed at *m*/z 646.6 and its CO-loss products (see SI). Other authors reported using $[Fe_3(CO)_9(\mu\text{-}CO)\{\mu_3\text{-}PFe(CO)_4\}]^-$ as the $[Et_4N]^+$ salt but provided no details of the synthesis.[42]

$$[Et_4N]_2[Fe_4(CO)_{13}] \xrightarrow[CH_2Cl_2,\ RT,\ 1\ h]{0.75\ eq.\ PCl_3} [Et_4N][\{Fe_3(CO)_9(\mu\text{-}CO)\}(\mu_3\text{-}PFe(CO)_4)]$$

80%‡

‡ Isolated Yield (Based on P) (9)

Interestingly, treatment of $[Et_4N]_2[Fe_4(CO)_{13}]$ in DCM with $AsCl_3$ in the same ratios as used for our synthesis of $[Fe_3(CO)_9(\mu\text{-}CO)\{\mu_3\text{-}PFe(CO)_4\}]$- yielded **II**, some $[\mathbf{V}]^-$, and a small amount of $Fe_3(CO)_{12}$ and $Fe(CO)_5$ which could be removed under vacuum. Although some $[\mathbf{V}]^-$ did form, the absence of $[\mathbf{III}]^{2-}$ from the product mixture was intriguing as the corresponding reaction with $SbCl_3$ yielded the Sb-analog of $[\mathbf{III}]^{2-}$ as the majority product.[41] Thus, the mixture of products arising from the treatment of $[Et_4N]_2[Fe_4(CO)_{13}]$ with PCl_3, $AsCl_3$, and $SbCl_3$, respectively were quite different and may be attributable to the ease of reduction of the heavier main group elements. The speculation is that the pathway for the heavier elements is primarily initiated by a redox reaction that results in more fragmentation and recombination of these fragments. The exact nature of the intermediates, however, remains unknown. In spite of the reaction in **Equation 9** appearing to be a nucleophilic displacement of halide from EX_3, the reaction is substantially more complicated and the fact that there are four Fe atoms in both starting material and product is likely coincidental given the stoichiometry of the reaction which requires excess metal carbonyl starting material.

STRUCTURAL STUDIES

Structure of [Et4N][IV]

The anion $[\mathbf{IV}]^-$ (**Figure 1**) is closely related to $[\mathbf{I}]^{2-}$, the main differences being the introduction of an Fe-Fe bond, bridging hydride ligand, and shift of a terminal CO to a bridging position. In $[Et_4N]_2[\mathbf{I}]$, the average Fe-As bond is 2.465(9) Å, which is much longer than the average Fe-As bond distance of 2.371(3) Å observed in $[Et_4N][\mathbf{IV}]$, likely due to the relaxation in steric crowding about the central arsenic atom accompanying the formation of the Fe-Fe bond. The average Fe-As-H1 angle in $[Et_4N]_2[\mathbf{I}]$ is 102.3(2)° while the corresponding angle in $[Et_4N][\mathbf{IV}]$ is 107.3(7)° reflecting a more tetrahedral arsenic, again due to less steric crowding in $[\mathbf{IV}]^-$. The Fe3-As bond distance of 2.3722(4) Å in $[\mathbf{IV}]^-$ is closer to the As-$Fe(CO)_4$ distance in $[Et_4N]_2[\mathbf{III}]$ of 2.400(0) Å than to the As-$Fe(CO)_4$ (Fe4 -As1) length of 2.3369(8)Å in $[\mathbf{V}]^-$ This could be due to less steric strain in $[\mathbf{V}]^-$ as compared to the analogous distances in $[\mathbf{III}]^{2-}$ and $[\mathbf{IV}]^-$. Additionally, the hybridization at the main group atom in $[\mathbf{III}]^{2-}$ could force a larger s-character in the E-$Fe(CO)_4$ bond as seen previously for molecules in this class.[37]

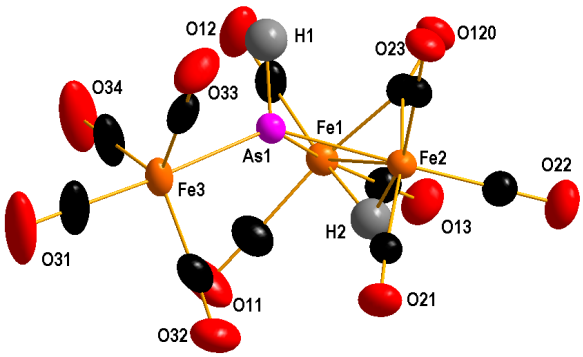

Figure 1. Diagram of $[\mathbf{IV}]^-$; Anisotropic displacement ellipsoids are shown at 50% probability.

The Fe1-Fe2 bond distance of 2.5981(5) Å is consistent with the Fe-Fe bond in an $Fe_2(CO)_6(\mu\text{-}CO)(\mu\text{-}H)$ unit (average 2.5869(16) Å, including the analogous distance in $[\mathbf{VII}]^-$).[44–47] References **44-47** represent the only examples of an $\{Fe_2(CO)_7H\}$ moiety in the Cambridge Structural Database other than $[\mathbf{VII}]^-$. The Fe-H and Fe-(μ-CO) bonds are relatively symmetric and consistent with the literature.[44–47] The bridging C=O bond length of 1.180(3) Å in $[Et_4N][\mathbf{IV}]$ is consistent with that of those bridging the other literature$\{Fe_2(CO)_7H\}$ compounds (average 1.183(14) Å) but longer than that observed in $[\mathbf{VII}]^-$ (1.132(4) Å).[44–47]

The presence of the arsenic hydride and bridging hydride are confirmed by ^{1}H NMR spectroscopy. The arsenic hydride signal was observed at 1.51 ppm, similar to the hydride signal in AsH_3 of 1.786 in d_3-MeCN.[48] The bridging hydride signal at -9.98 ppm is broad and in agreement with the broad -9.64 signal observed for the hydride in $(\mu\text{-}H)Fe_2(CO)_6(\mu\text{-}CO)[\mu\text{-}P(OH)\{CH(SiMe_3)_2\}]$ by Arif et al.[47] Metallated arsenic hydride moieties are relatively rare. Only five other examples (including $[\mathbf{I}]^{2-}$) are known in the Cambridge Structural Database[49–51] and two further compounds were identified as possessing an arsenic-hydrogen bond by ^{1}H NMR.[52,53] The range of chemical shifts of the As-H bond in these metallated species is -2 to 2.6 ppm with the signal at 15.08 ppm for $(\mu\text{-}AsH)\{Mn(Cp)_2(CO)_2\}_2$ reported by Hermann et al. being an outlier.[49–53] The As-H moiety possesses intrinsic reactivity and can be used as a gateway for further chemistry.

Structures of AsM_4 Compounds

There are two common coordination environments found for

As in its metal carbonyl cluster compounds containing four metals. The first is based on a tetrahedral M_3As unit with an additional metal fragment attached to the lone pair on As. We refer to this structure as spiked-tetrahedral arrangement. The second common geometry is a spirocyclic assembly in which the As is bound to two M_2 units each containing a M-M bond. For both the homometallic iron and heterobimetallic Fe-Mn clusters, the observation of both spirocyclic and spiked tetrahedral structures leads us to postulate a common tetrametallic intermediate that possesses only one M-M bond (**Scheme 6**). Such EM_4 compounds containing only one M-M bond are known in the literature.[54–57] Such an intermediate could close in one of two directions. The two non-bonded $M(CO)_x$ units could lose one CO with formation of a M-M bond to give the spirocyclic structure, alternatively, an $M(CO)_x$ unit could form two M-M bonds with the existing M_2 unit and loss of two carbonyl ligands to produce the spiked tetrahedral structure. Closure to either the spirocyclic or spiked tetrahedral structure is likely governed by electronic requirements (the 18-electron rule).

Table 1: Selected Bond Lengths and Angles of [**V**]$^-$, [V**III**]$^-$, and P and Sb Analogs

		[**V**]$^-$, E=As	[**VIII**]$^-$, E=As	$[Ph_4P][Fe_3(CO)_9(\mu\text{-}CO)(\mu_3\text{-}PFe(CO)_4)]$[40]	$[Et_4N][Fe_3(CO)_9(\mu\text{-}CO)(\mu_3\text{-}SbFe(CO)_4)]$[41]
Bonds (Å)	Fe(1)-E(1)	2.3369(8)	2.3222(9)	2.245(3)	2.515(2)
	Fe(2)-E(1)	2.3380(6)	2.3204(9)	2.237(3)	2.518(3)
	Fe(3)-E(1)	2.2611(6)	2.2734(10)	2.156(3)	2.460(3)
	M(4)-E(1)	2.3275(8), M=Fe	2.4157(9), M=Mn	2.234(3), M=Fe	2.481(3), M=Fe
	Fe(1)-Fe(2)	2.6166(7)	2.6306(10)	2.593(2)	2.660(3)
	Fe(1)-Fe(3)	2.6553(7)	2.6407(12)	2.620(2)	2.680(3)
	Fe(2)-Fe(3)	2.6498(9)	2.6623(11)	2.640(2)	2.685(4)
	Avg. Fe-Fe	2.641(21)	2.645(16)	2.618(24)	2.675(13)
	Avg. Fe-Fe Unbridged	2.653(4)	2.652(15)	2.630(14)	2.683(15)
	C(120)-O(120)	1.173(3)	1.157(6)	1.155(13)	1.146(2)
	Mn(4)-Br(1)	—	2.5178(10)	—	—
Angles (°)	M(4)-E(1)-Fe(1)	139.62(2), M=Fe	136.98(4), M=Mn	134.4(1)	143.3(1)
	M(4)-E(1)-Fe(2)	136.507(18), M=Fe	136.73(3), M=Mn	134.7(1)	134.4(1)
	M(4)-E(1)-Fe(3)	139.925(18), M=Fe	141.61(4), M=Mn	141.1(1)	146.5(1)
	E(1)-Mn(4)-Br(1)		89.67(3)		

Scheme 5. Possible intermediate closing to form either a spirocyclic or spiked tetrahedral structure.

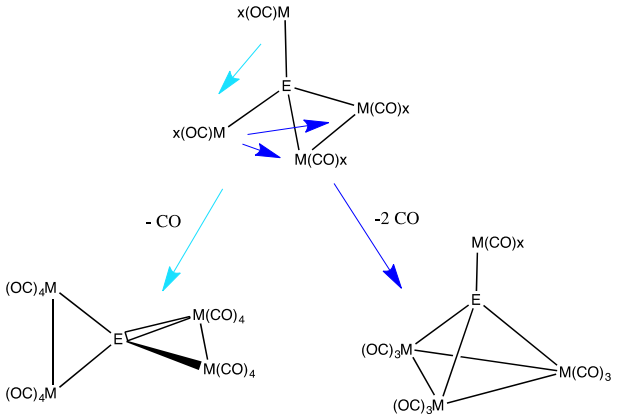

Structural comparisons of the Spiked Tetrahedral Clusters

The M_3E units in the spiked tetrahedral structures possess 48 electrons giving rise to metal centers that obey the 18-electron rule. $Fe_3(CO)_{12}$ can be viewed as the prototype cluster on which $[Et_4N][\mathbf{V}]$, $[Et_4N][\mathbf{VI}]$, $[Et_4N][\mathbf{VIII}]$, and **IX** are based. Replacement of three carbonyls with As^{3-} results in an isoelectronic $[Fe_3(CO)_9As]^{3-}$ core in which six electrons are donated to the metal framework while the As atom retains a lone pair of electrons. Two of these electrons can be replaced with the neutral bridging CO to give a $[Fe_3(CO)_9(\mu\text{-}CO)(\mu_3\text{-}As)]^-$, while protonation would produce the series $[(\mu\text{-}H)Fe_3(CO)_9(\mu_3\text{-}As)]^{2-}$, $[(\mu\text{-}H)_2Fe_3(CO)_9(\mu_3\text{-}As)]^-$ and $(\mu\text{-}H)_3Fe_3(CO)_9(\mu_3\text{-}As)$. Anions $[\mathbf{V}]^-$ and $[\mathbf{VIII}]^-$ contain $[Fe_3(CO)_9(\mu\text{-}CO)(\mu_3\text{-}As)]^-$ whereas $[\mathbf{VI}]^-$ and **IX** contain the $[(\mu\text{-}H)_2Fe_3(CO)_9(\mu_3\text{-}As)]^-$ moiety (**Figure 2**). As is common with these two classes, the H-bridged M-M bonds are the longest, the CO-bridged bonds are the shortest, with non-bridged bonds being intermediate between these two extremes.

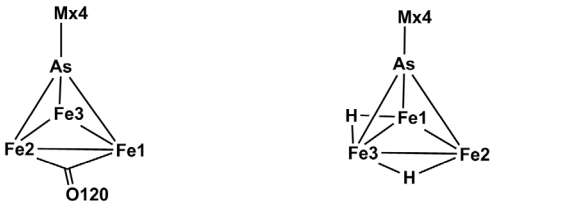

$\{Fe_3(CO)_9(\mu\text{-}CO)\}As\{M_X(CO)_Y\}$ M=Fe, Mn

$\{Fe_3(CO)_9(\mu\text{-}H)_2\}As\{M_X(CO)_Y\}$ M=Fe, Mn

Figure 2. The two general structural motifs of the "spiked" tetrahedral complexes

The $[Fe_3(CO)_9(\mu\text{-}CO)AsML_n]^{x-}$ Clusters

Phosphorus and antimony derivatives isostructural with $[Et_4N][\mathbf{V}]$ are known.[40,41] As one might expect, the pattern of bond lengths and angles in each of the three clusters is similar, although not identical. **Table 1** ontains a comparison of key bond lengths and angles of $[Et_4N][\mathbf{V}]$, $[Et_4N][\mathbf{VIII}]$ (**Figure 3**), and the structurally analogous $[Ph_4P][Fe_3(CO)_9(\mu\text{-}CO)(\mu_3\text{-}PFe(CO)_4)]$ and $[Et_4N][Fe_3(CO)_9(\mu\text{-}CO)(\mu_3\text{-}SbFe(CO)_4)]$.[40,41]

The asymmetry introduced by the bridging carbonyl, which shortens one of the Fe-Fe bonds, is reflected in a distortion of the iron-capped tetrahedron. In each cluster, the shortest Fe-E bond lies opposite the bridging carbonyl as the pnictogen is pushed away from the relatively higher electron density between the CO-bridged irons. The iron-capping each of the tetrahedron is consequently tilted slightly toward the bridging CO moiety. The average unbridged Fe-Fe bond distance in the tri-iron-moiety of $[\mathbf{V}]^-$ is 2.653(4) Å, intermediate to the corresponding distance in the phosphorus (2.630(14) Å) and antimony compounds (2.683(15) Å). The CO-bridged Fe1-Fe2 distance of 2.6166(7) Å is very similar to that of the P-analog at 2.620(2) Å but shorter than the 2.660(3) Å of the Sb-analog,[40,41]differences which can largely be explained by the similar atomic radii of arsenic and phosphorus at 1.20 Å and 1.09 Å, respectively, as compared to that of antimony at 1.40 Å.[58] The mean Fe-Fe bond distance in the tri-iron moiety of 2.641(21) Å is slightly longer than in the phosphorus analog (2.618(24) Å) and slightly shorter than the same distance in the antimony analog (2.675(13) Å), consistent with the sizes of the main group elements. The mean Fe-Fe bond distance in the structurally similar $\{Cr(CO)_5\}_2(\mu_4\text{-}As)_2\{Fe_3(CO)_9\}$[32] is significantly longer at 2.688(2) Å, likely attributable to the lack of the bridging CO which has a shortening effect when present.

The Fe4-As1 length of 2.3275(8) Å, is markedly shorter than the As-$Fe(CO)_4$ bond length in $[\mathbf{III}]^{2-}$ of 2.400(0) Å[37] and the Fe3-As1 distance of 2.3722(4) Å in $[\mathbf{IV}]^-$. This could be due less steric strain in $[\mathbf{V}]^-$ as compared to the analogous distances in $[\mathbf{III}]^{2-}$ and $[\mathbf{IV}]^-$. Additionally, the hybridization at the main group atom in $[\mathbf{III}]^{2-}$ forces a larger s-character in the E-$Fe(CO)_4$ bond.[59]

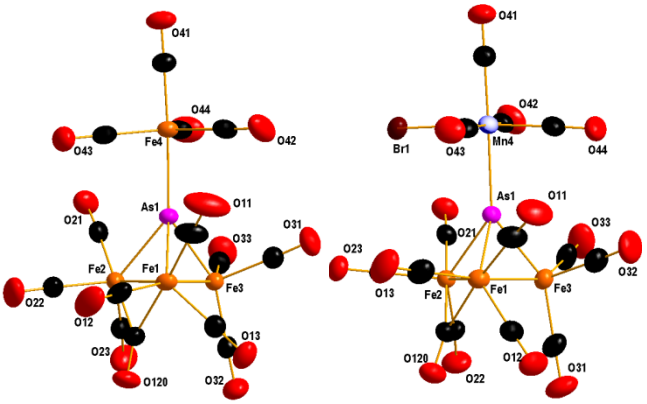

Figure 3. Diagram of [V]- (left) and [VIII]- (right); anisotropic ellipsoids shown at 50% Probability

The pattern of bond lengths and angles in $[\mathbf{VIII}]^-$ matches that of $[\mathbf{V}]^-$. Like $[\mathbf{V}]^-$, the bridging CO causes the cluster to be asymmetric with the arsenic atom being closer to Fe3, the Mn tilting toward Fe1-Fe2. As one might expect, the bond lengths and angles in the Fe_3As core are nearly identical. The mean Fe-Fe bond distance for $[\mathbf{VIII}]^-$ is 2.645(16) Å, nearly identical to the 2.641(21) Å observed in $[\mathbf{V}]^-$. The CO-bridged

Fe1-Fe2 distance is slightly longer in [**VIII**]$^-$ than that of the same distance in [**V**]$^-$, perhaps due to steric effects accompanying the $Mn(CO)_4Br$ moiety's tilt toward the Fe1-Fe2 bond. The average unbridged Fe-Fe distance in [**VIII**]$^-$ is 2.652(15) Å, compared with the same metric in [**V**]$^-$ of 2.653(4) Å. The As-Mn bond of 2. 4157(9) Å is consistent with an Mn-As bond (avg 2.451(155) Å)).[32,60,61]

The $[H_2Fe_3(CO)_9AsML_n]^{x-}$ Clusters

Compounds $[Et_4N]$[**VI**] and **IX** (**Figure 4**) are built on the $[H_2Fe_3(CO)_9As]^-$ core. Replacement of the bridging CO of [**V**]$^-$ with two bridging hydride ligands results in [**VI**]$^-$. For [**VIII**]$^-$ not only has the bridging CO been replaced but the $\{Mn(CO)_4Br\}$ has been converted into a $Mn(CO)_5^+$ unit in order to obtain **IX**. Consequently, **IX** is electron precise as a neutral molecule. In [**VI**]$^-$ the lone pair on As is attached to an $\{Fe(CO)_4\}$ group, a structure shared with $[Et_4N][(\mu\text{-}H)_2Fe_3(CO)_9\{\mu_3\text{-}SbFe(CO)_4\}]$.[54] **Table 2** gives a comparison of selected bond lengths and angles for the three clusters. The effect of the two bridging hydrides is the same for each cluster: the arsenic tilts slightly away from the bridging hydrides, specifically the iron atom that shares both bridging hydrides. The presence of the hydrides lengthens the bonds across which they span. The unbridged Fe1-Fe2 in [**VI**]$^-$ distance is 2.681(6) Å; the average bridged Fe-Fe distance is 2.725(6) Å. These distances are shorter than those of the Sb cluster 2.7339(10) Å and 2.780(3) Å respectively, and nearly identical to those of **IX** at 2.6869(16) Å and 2.728(2) Å respectively. The distance from the capping iron to As1 is 2.3443(91) Å, similar to that of the corresponding distance in [**V**]- of 2.3275(8) Å. The average Fe-Fe distance is 2.710(23) Å for [**VI**]$^-$ compared with 2.714(23) Å in **IX**.

Table 2: Selected Bond Lengths and Angles of [**V**]$^-$, [**VIII**]$^-$, and P and Sb Analogs

		[**V**]$^-$, E=As	[**VIII**]$^-$, E=As	$[Ph_4P][Fe_3(CO)_9(\mu\text{-}CO)(\mu_3\text{-}PFe(CO)_4)]$[40]	$[Et_4N][Fe_3(CO)_9(\mu\text{-}CO)(\mu_3\text{-}SbFe(CO)_4)]$[41]
Bonds (Å)	Fe(1)-E(1)	2.3369(8)	2.3222(9)	2.245(3)	2.515(2)
	Fe(2)-E(1)	2.3380(6)	2.3204(9)	2.237(3)	2.518(3)
	Fe(3)-E(1)	2.2611(6)	2.2734(10)	2.156(3)	2.460(3)
	M(4)-E(1)	2.3275(8), M=Fe	2.4157(9), M=Mn	2.234(3), M=Fe	2.481(3), M=Fe
	Fe(1)-Fe(2)	2.6166(7)	2.6306(10)	2.593(2)	2.660(3)
	Fe(1)-Fe(3)	2.6553(7)	2.6407(12)	2.620(2)	2.680(3)
	Fe(2)-Fe(3)	2.6498(9)	2.6623(11)	2.640(2)	2.685(4)
	Avg. Fe-Fe	2.641(21)	2.645(16)	2.618(24)	2.675(13)

	Avg. Fe-Fe Unbridged	2.653(4)	2.652(15)	2.630(14)	2.683(15)
	C(120)-O(120)	1.173(3)	1.157(6)	1.155(13)	1.146(2)
	Mn(4)-Br(1)	—	2.5178(10)	—	—
Angles (°)	M(4)-E(1)-Fe(1)	139.62(2), M=Fe	136.98(4), M=Mn	134.4(1)	143.3(1)
	M(4)-E(1)-Fe(2)	136.507(18), M=Fe	136.73(3), M=Mn	134.7(1)	134.4(1)
	M(4)-E(1)-Fe(3)	139.925(18), M=Fe	141.61(4), M=Mn	141.1(1)	146.5(1)
	E(1)-Mn(4)-Br(1)		89.67(3)		

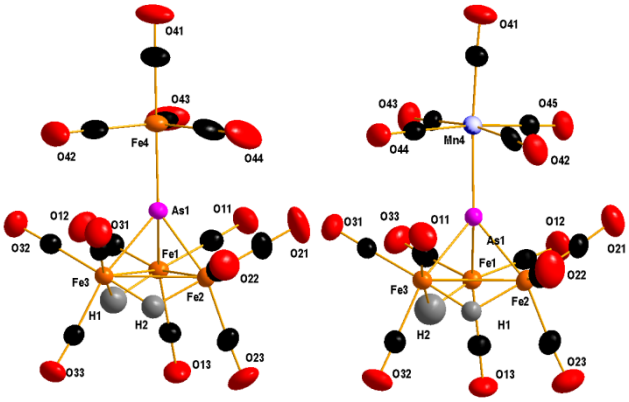

Figure 4. Diagram of [**VI**]$^-$ (left) and **IX** (right); anisotropic displacement ellipsoids shown at 50% probability.

Structural comparison of the "spirocyclic" complexes ([Et$_4$N][VII] and X)

[**VII**]$^-$ and **X** belong to a general class of metal carbonyl clusters in which two M_2 units, each containing a metal-metal bond, are bound to a central main group atom, a well-known configuration (**Figure 5**).[62–74]

Both [**VII**]$^-$ and **X** contain three Fe atoms and one Mn atom divided between two M_2 fragments (**Figures 6 and 8**). [**VII**]$^-$ and **X** each possess an $MnFe(CO)_8$ fragment as well as a diiron unit which is either $(\mu\text{-H})Fe_2(CO)_6(\mu\text{-CO})^-$ or $Fe_2(CO)_8$ for [**VII**]$^-$ and **X** respectively. In a spirocyclic configuration, the As atom donates five electrons to the two metal fragments. The $FeMn(CO)_8$ fragment in each species requires three electrons, while the diiron units in [**VII**]$^-$ and **X** require three and two electrons respectively. In [**VII**]$^-$, the negative charge supplies the remaining electron to satisfy the 18-electron rule.

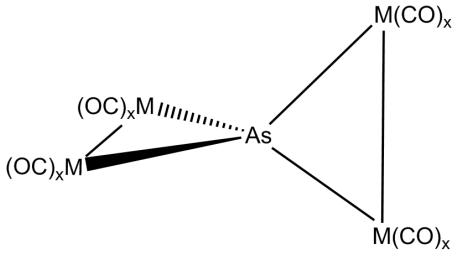

Figure 5. General Spirocyclic Metal Carbonyl

Anion [**VII**]$^-$ consists of two M_2 fragments, one of which possesses a bridging hydride that was easily located and refined crystallographically. In [**VII**]$^-$ the manganese atoms could be localized to the $M_2(CO)_8$ fragment based on crystallographic refinement and the fact that $\{FeMn(CO)_6(\mu\text{-CO})(\mu\text{-H})\}$ is an unknown moiety. Also, based on the similarity to [Et_4N][**IV**] we believe it to be an Fe_2 fragment. This is the first time an $\{Fe_2(CO)_7H\}$ moiety has been observed in a spirocyclic molecule. The M3 and M4 positions in the structure were modeled as a mixture of iron and manganese with the exact composition allowed to refine with a free variable, which refined to a ~50% manganese occupancy at each site. The cluster's formulation is also supported by ESI-MS data; the parent $[HAsFe_3Mn(CO)_{15}]^-$ is observed at m/z = 718.6 with its CO-loss products (See SI).

The CO-bridged Fe-Fe bond is short at 2.6051(18) Å although consistent with the other known examples of an $\{Fe_2(CO)_7H\}$ group (average 2.585(15) Å including that of [**IV**]$^-$).[44–47] The Fe-Mn bond is much longer at 2.8191(15) Å though consistent with other M-M bonds in $M_2(CO)_8$ spirocyclic environments (average: 2.816(44) Å).[60,62-70] The average arsenic bond distance to the $\{Fe_2(CO)_7H\}$ fragment is 2.377(6) Å while the As-Fe/Mn distances are slightly shorter at 2.3647(2) Å, likely due to less strain in the $FeMn(CO)_8$ moiety. The bond distance of the C=O bond in the bridging carbonyl (C120-O120) of 1.132(4) Å appears to be shorter than the respective bridging carbonyls of the other known $\{Fe_2(CO)_7H\}$ groups (average of 1.182(12) Å).[44–47]

Given that the solid state structure of [**VII**]$^-$ has the Fe and Mn statistically disordered, two isomers should exist based

on the relative orientation of the bridging carbonyl with respect to a particular metal atom. The ^{1}H NMR spectrum of this compound (**Figure 7**)shows a broad signal consistent with a bridging hydride in an $\{Fe_2(CO)_7H\}$ group at -8.7 ppm in d_6-acetone.[47] Given that the hydride can be either *trans* or *cis* with respect to the manganese in the $M_2(CO)_8$ fragment, two signals should be observed.

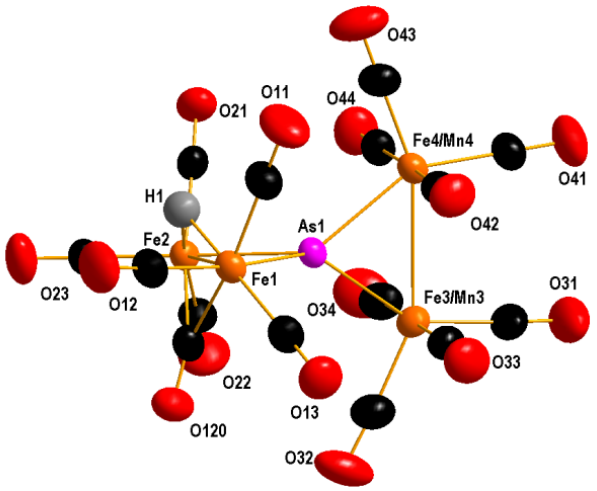

Figure 6. Diagram of [**VII**]$^-$; anisotropic displacement ellipsoids shown at 50% Probability

Only one signal is observed at room temperature, but cooling results in broadening, coalescence, and ultimately the resolution into two distinct peaks by -40 °C. The coalescence temperature is between room temperature and -10 °C. This implies ΔG of activation of between 51 and 57 kJ/mol.[75]

There are three possible ways in which the positions of the H and bridging CO can equilibrate with respect to the positions of the Mn atom (**Scheme 7**). One possibility is that one of the M_2 units could rotate with respect to the other. This is most likely a higher energy process compared to another option involving bridge-terminal interconversion of the H and μ-CO ligands, with these ligands reforming the bridging configurations on the opposite sides of the Fe_2 group. Furthermore, a reviewer suggested the mechanism of interconversion might be through opening of one of the M-As bonds, rotation of the diiron unit about the remaining M-As bond and reformation of the M_2As triangle to give the other isomer. We would point out that in the related compound $Pb\{Fe_2(CO)_8\}_2$, the carbonyls were shown to be fluxional down to the lowest temperature that could be achieved while maintaining Pb-C coupling throughout the process, indicating that the Pb-Fe bonds are not broken in that process.[76]

Scheme 7. Mechanism for isomer interconversion of [VII]$^-$. Terminally bound COs on the Fe_2 fragment could also scramble with the μ-CO in this process.

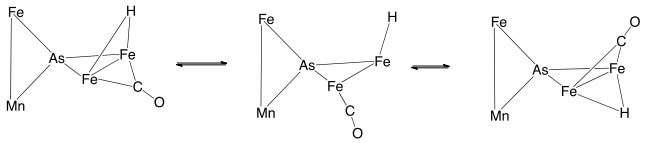

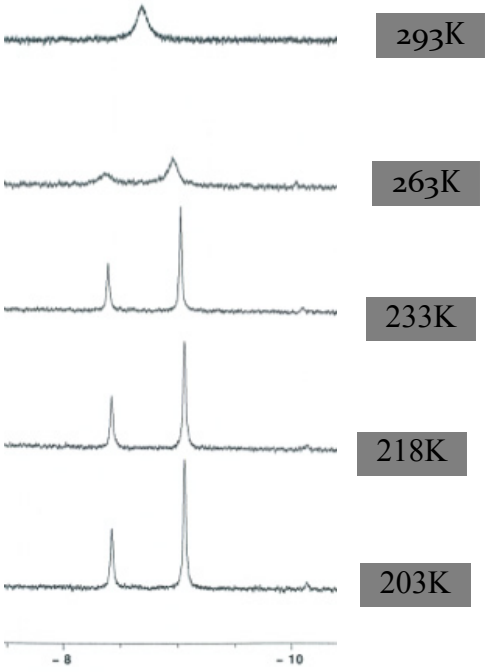

Figure 7. VT ^{1}H-NMR Spectra of [**VII**]$^-$ in the bridging hydride region.

The ^{1}H NMR spectrum shows a group of signals around -22 ppm present in the same ratios even when starting from crystalline material that gave acceptable elemental analyses. These signals exist in approximately a 1:5 ratio relative to the hydride signal at -8.7 ppm. Moreover, the secondary signals were present irrespective of solvent; samples were prepared in d_6-acetone, d_3-acetonitrile, and d_8-THF. These probably represent some minor impurities that most likely contain bridging hydride ligands on M_3 triangles. ESI-MS of the product shows two minor peaks at m/z = 793.8 and 819.8 that are consistent with this interpretation. The 793.8 peak is consistent with the mono-deprotonated $[[Et_4N][Fe_2Mn(CO)_9(\mu\text{-}H)_2\{\mu_3\text{-}AsFe(CO)_4\}]]^-$ anion which would correspond to an electron precise capped tetrahedron with a postulated parent compound $[Et_4N][Fe_2Mn(CO)_9(\mu\text{-}H)_3\{\mu_3\text{-}AsFe(CO)_4\}]$, while the 819.8 peak fits with the formulation$[[Et_4N][\{Fe_3(CO)_9\}(\mu_3\text{-}AsMn(CO)_5]]^-$, also an electron-precise spiked tetrahedral structure that could arise from the presence of $[Et_4N][\{Fe_3(CO)_9(\mu\text{-}H)\}\{\mu_3\text{-}AsMn(CO)_5\}]$. The former would have two proton signals in a 2:1 ratio as there are two different ^{1}H environments in an $\{Fe_2Mn(CO)_9(\mu\text{-}H)_3\}$ moiety. We assign the peaks at -21.80 and -20.85 ppm to this species, the major impurity. The latter compound that corresponds to a deprotonated version of **IX** should have a single signal and the most likely assignment is -24.25 ppm. This is similar to the -23.69 ppm shift observed for compound IX. This leaves four very small peaks (<1% of the sample) unassigned that most likely correspond to other deprotonated forms of these compounds.

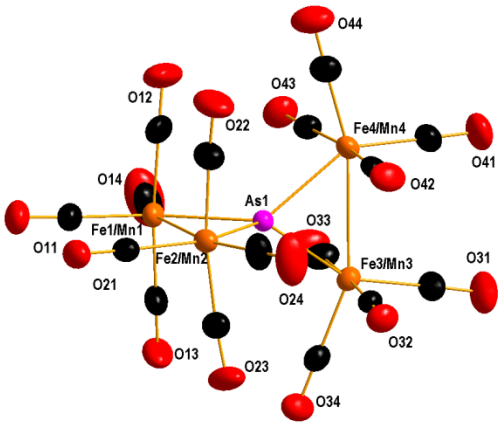

Figure 8. Diagram of **X** anisotropic displacement ellipsoids shown at 50% Probability

Compound **X** exists as two polymorphs A and B, with B apparently possessing small void containing highly disordered MeCN. The fundamental structures are the same; however there are some differences in the bond distances (Table S7, S10). The data for polymorph B were less precise. Two $M_2(CO)_8$ fragments are bound to a central arsenic atom, and the structure was modeled with the Fe and Mn atoms statistically disordered over the four metal atom positions ($Fe_{0.75}Mn_{0.25}$) for both polymorphs. **X** is a neutral molecule and obeys the 18-electron rule. The average M-M bond is 2.821(25) Å, similar to 2.816(44) Å, the average M-M bond distance for a variety of spirocyclic $EM_2(CO)_8$ compounds where M were first row transition metals.[64,66–74] It was also similar to the 2.8191(15) Å observed in [**VII**]$^-$. **Table 3** gives a comparison of **X** to all known $E\{Fe_2(CO)_8\}_2$ clusters where E is a main group atom (E = Si, Ge, In, Sn, Pb). **X**, which contains As, has bond lengths and angles most similar to the spirocycles containing Ge and Si. This can be explained by examination of the respective covalent atomic radii of the elements. As, Ge, and Si have similar radii at 1.20, 1.20, and 1.14 Å, respectively. Consequently their bond lengths and angles are nearly identical. Furthermore, the spirocycles containing In, Sn, and Pb have closely matching bond lengths and angles and covalent atomic radii of 1.40, 1.42, and 1.45 Å, respectively. Thus, among the spirocycles, atomic radius of the central main group atom has a large impact on the overall size of the respective cluster.

CONCLUSIONS

A systematic investigation of the reactivity of $[Et_4N]_2$[**I**] has produced a series of new homometallic iron and heterometallic iron/manganese clusters containing arsenic, several of which can be obtained in high yield starting with the easily prepared $[Et_4N]_2$[**I**]. The syntheses reported here are relatively safe as long as proper Schlenk technique is observed and are readily scalable. The starting material for each reaction, $[Et_4N]_2$[**I**] is versatile, nonvolatile, and inexpensively made. The observed reaction products from this starting material can be rationalized by pathways that involve oxidation and/or hydrogen atom, hydride ion or hydronium ion abstraction, depending upon the reagent employed. These pathways may compete with each other resulting in a mixture of products that to some extent may be tailored by proper choice of the reaction conditions. Furthermore, as metal-metal bond formation is seldom predictable, these results help answer the question of when and where in a given cluster metal-metal bond formation will occur, in particular for arsenic-containing metal carbonyl clusters, but may yield insight into the outcomes of similar processes for other mixed main-group metal carbonyl clusters.

Our oxidation experiments with [**I**]$^{2-}$ point to cleavage of the hydride forming a radical, a process which promotes for acceptance of an $H^\bullet$ or $Mn(CO)_5^\bullet$ fragment and protonation may give rise to [**IV**]$^-$ and [**VII**]$^-$, the latter of which exists as two distinct isomers at low temperature in solution and in the solid state. Abstraction of the hydride has two possible outcomes such as observed in the production of [**V**]$^-$ and [**III**]$^{2-}$, which suggests that the intermediate, a radical species, can combine with other mononuclear metal fragments present in the reaction or with itself to give higher nuclearity species. In the case of the $Mn(CO)_4$LBr product ([**VIII**]$^-$), it is likely that simple substitution of CO by a complex cluster donor occurs.

The bimetallic iron/manganese clusters [**VII**]$^-$, [**VIII**]$^-$, **IX**, and **X** contain arsenic completely ligated by metal. Of these, [**VII**]$^-$ and **X** are obtained in high yield with [**VII**]$^-$ possessing a great deal of reactivity and **X** being a neutral bimetallic molecule with a simple carbonyl ligand environment. The overall route from [**I**]$^{2-}$ to compound **X** is convenient and straightforward.

Treating [**VII**]$^-$ with base with expulsion of $[Mn(CO)_5]^-$ presumably unmasked an $[Fe_3(CO)_9(\mu\text{-CO})(\mu_3\text{-As})]^-$ unit. It is possible that [**VII**]$^-$ could serve as a source of this unit in further cluster building. There are several starting materials closely related to [**I**]$^{2-}$ for which similar chemistry may be possible (e.g. $[HE\{Cr(CO)_5\}_3]^{2-}$ E = (As/Sb), $[HSb\{Fe(CO)_4\}_3]^{2-}$, etc.) creating possibilities for further heterometallic complexes.[50,76] The bimetallic iron/manganese clusters [**VII**]$^-$, [**VIII**]$^-$, **IX**, and **X** contain arsenic completely ligated by metal. Of these, [**VII**]$^-$ and **X** are obtained in high yield with [**VII**]$^-$ possessing a great deal of reactivity and **X** being a neutral bimetallic molecule with a simple carbonyl ligand environment. The overall route from [**I**]$^{2-}$ to compound **X** is convenient and straightforward.

***Table 3*:** Selected Bond Lengths and Angles of E{$Fe_2(CO)_8$}$_2$ E={Si, Ge, In, Sn, and Pb} and **X** (average of both polymorphs)

	Si{$Fe_2(CO)_8$}$_2$	Ge{$Fe_2(CO)_8$}$_2$	[In{$Fe_2(CO)_8$}$_2$]$^-$	Sn{$Fe_2(CO)_8$}$_2$	Pb{$Fe_2(CO)_8$}$_2$	X
Average Fe-Fe (Å)	2.7925(7)	2.823(12)	2.87(0)	2.900(2)	2.901(15)	2.821(25)
Average **E**-Fe (Å)	2.347(4)	2.408(21)	2.54(1)	2.627(1)	2.620(16)	2.369(8)
Mean Fe-**E**-Fe (Å)	73.05(7)	71.8 (3)	68.9(0)	67.0(1)	67.2(4)	73.1(9)
Average Fe-Fe-**E** (°)	53.5(1)	54.1(6)	55.5(4)	56.5(1)	56.4(6)	53.4(5)
Covalent Atomic Radius[54] of **E** (Å)	1.14	1.20	1.40	1.42	1.45	1.20
Reference	[67]	[70]	[75]	[72]	[76]	this work

Treating [**VII**]$^-$ with base with expulsion of [$Mn(CO)_5$]$^-$ presumably unmasked an [$Fe_3(CO)_9(\mu\text{-}CO)(\mu_3\text{-}As)$]$^-$ unit. It is possible that [**VII**]$^-$ could serve as a source of this unit in further cluster building. There are several starting materials closely related to [**I**]$^{2-}$ for which similar chemistry may be possible (e.g. [HE{$Cr(CO)_5$}$_3$]$^{2-}$ E = (As/Sb), [HSb{$Fe(CO)_4$}$_3$]$^{2-}$, etc.) creating possibilities for further heterometallic complexes.[50,76]

Compound **X** is very nearly of the composition required for it to be an SSP for the half-Heusler alloy $Fe_{2-x}Mn_xAs_yP_{1-y}$. If phosphorus can be introduced easily, the resulting cluster could be evaluated as such an SSP. If successful $Fe_{2-x}Mn_xAs_yP_{1-y}$ with its giant magnetocaloric effect at near ambient could be accessed at mild temperatures conveniently and potentially as a nanomaterial. Efforts to introduce phosphorus to **X** are underway.

EXPERIMENTAL

General Considerations

All reactions were performed under dry, oxygen-free argon according to standard Schlenk technique. The solvents tetrahydrofuran, dichloromethane, ethyl ether, toluene, and hexane were dried using a Pure Process Technology solvent purification system and degassed prior to use. Compounds [Et_4N]$_2$[HAs{$Fe(CO)_4$}$_3$], [Et_4N][$HFe(CO)_4$], and $Mn(CO)_5Br$ were prepared according to literature methods.[29,77,78] [Et_4N]$_2$[$Fe_4(CO)_{13}$] was prepared by a modified literature method in which [Et_4N]Br was used in place of [PPN]Cl.[79] [CPh_3][BF_4] and trifluoromethanesulfonic acid were obtained from Sigma Aldrich and used without further purification. Triethylamine was obtained from Sigma Aldrich, dried over KOH, and distilled under argon. $AgPF_6$ was obtained from Strem and used without further purification. IR measurements were obtained using a Perkin Elmer Spectrum Two FTIR spectrometer. ^{1}H and ^{31}P NMR data were recorded on a 500 MHz Bruker spectrometer (202 MHz for ^{31}P). ESI-MS data was collected on a Bruker Daltoniks microTOF ESI/MS coupled with an Agilent 1200 HPLC. Elemental Analyses were performed by Galbraith Laboratories Inc.

Synthesis of Compounds

Synthesis of [Et_4N][HAs{$Fe_2(CO)_6(\mu\text{-}CO)(\mu\text{-}H)$}{$Fe(CO)_4$}], [$Et_4N$][IV]: Method A) To a solution of 1.0 g (1.2 mmol) of [Et_4N]$_2$[**I**] dissolved in 20 mL THF was added 0.30 g (1.2 mmol) $AgPF_6$ in 30 mL THF over five minutes by cannula in the dark at room temperature. The resulting deep brown-orange solution was stirred in the dark for 30 minutes, and then the solvent was removed *in vacuo*. 60 mL of diethyl ether was added and the mixture allowed to stand overnight. The following day, the solution was filtered and stored in the freezer at -10 °C giving rise to a mixture of crystals of [Et_4N][**IV**] and [Et_4N][**V**]. The crystals of [**IV**]$^-$ were ruby-red prismatic blocks. Yield of [Et_4N][**IV**]: 98 mg, 12% (based on As)

Method B) To a solution of 1.0 g (1.2 mmol) of [Et_4N]$_2$[**I**] and 0.7 g (2.4 mmol) [Et_4N][$HFe(CO)_4$] dissolved in 20 mL THF was added 0.60 g $AgPF_6$ (2.4 mmol) in 40 mL THF over five minutes by cannula in the dark at room temperature. The reaction was allowed to stir in the dark for 30 minutes followed by filtration, removal of the solvent *in vacuo*, treatment of the solids remaining after removal of the solvent with 200 mL diethyl ether, allowing the resulting solution to stand for 3 h at room temperature followed by filtration and storage at -10 °C. Crystals of of [Et_4N][**IV**] grew over the course of two weeks. Yield of [Et_4N][**IV**]: 580 mg, 71% (based on As)**.**

[Et_4N][**IV**] is extremely air-sensitive and should be stored under an inert atmosphere. [Et_4N][**V**] and [Et_4N]$_2$[**III**] were formed when this compound dissolved in MeCN was exposed to air. ν_{CO} (DCM) 2058 (vw), 2021 (vs), 1969 (m), 1949 (wsh), 1920. (w), 1761 (vw, br) cm^{-1}. Anal. Calcd. for $C_{19}H_{22}O_{11}NFe_3As$: C, 33.42 %; H, 3.25 %; N, 2.05 %. Found: C, 31.55%; H, 3.16%; N, 2.02%. Sample may be thermally unstable. ^{1}H NMR data (d_6-acetone, ppm): 3.497 (8H, *q*, *J* = 7.5 Hz), 1.509 (1H, *s*, As-H), 1.401 (12H, *t*, *J* = 7.5 Hz), -9.983 (1H, *s*). ESI-MS Data collected for method B ether extracted solids: *m/z* (%): 681.8 (1) [[Et_4N]{[**IV**]-H$^+$}]$^-$, 552.5 (7) [**IV**]$^-$, 522.5 (24) [**IV**]$^-$-CO –H_2, 494.5 (23) [**IV**]$^-$ -2CO - H_2, 466.5 (5) [**IV**]$^-$-3CO -H_2, 438.5 (5) [**IV**]$^-$ -4CO – H_2, 690.4 (2) [**V**]$^-$, 662.4 (1) [**V**]$^-$-CO, 634.4 (2) [**V**]$^-$ -2CO, 793.5 (1) [[Et_4N]{[**VI**]-H$^+$}]$^-$. Slightly soluble in ethyl ether; soluble in glyme, DCM, THF, acetone, and other polar organic solvents.

Synthesis of [Et_4N][$Fe_3(CO)_9(\mu\text{-}CO)(\mu_3\text{-}AsFe(CO)_4$], [$Et_4N$][V]: To a solution of compound [Et_4N]$_2$[**I**] (1.0 g, 1.2 mmol) dissolved in 20 mL of DCM was added [CPh_3][BF_4] (0.40 g, 1.2 mmol) dissolved in 20 mL of DCM over five minutes by cannula in the dark at room temperature. The resulting deep brown-orange solution was stirred in the dark for 30 minutes, and then 40 mL of toluene was introduced. After stirring for five minutes, the solvent volume was reduced until the solution was light orange and decanted away from a black precipitate. Then 60 mL of diethyl ether was added and the mixture allowed to stand overnight at room temperature. The solution was filtered and stored in the freezer at -10 °C giving rise to black, plate-like single crystals of [Et_4N][**V**]. Multiple treatments of ether were necessary to extract the product. Yield of [Et_4N][**V**]: 440 mg, 45% (based on As). ν_{CO} (DCM) 2056 (vw), 2028 (m), 2012 (s), 2000. (vs), 1965 (m, br), 1939 (w, br), 1794, (vw, br) cm^{-1}. Anal. Calcd. For $C_{22}H_{20}NO_{14}Fe_4As$: C, 32.20, H, 2.46, N, 1.71. Found (Average of the two samples submitted): C, 32.29%; H, 2.83%; N, 1.71%. ESI-MS Data collected for crystalline material: *m/z* (%): 690.4 (34) [**V**]$^-$, 662.4 (12) [**V**]$^-$ - CO, 634.4 (40) [**V**]$^-$ - 2CO, 578.4 (2) [**V**]$^-$-4CO,

550.4 (8) [**V**]$^-$-5CO, 522.5 (2) [**V**]$^-$ - 6CO, 494.5 (1) [**V**]$^-$ -7CO. Sparingly soluble in ethyl ether. Soluble in DCM, THF, and other polar solvents.

Synthesis of [Et$_4$N][Fe$_3$(CO)$_9$(μ-H)$_2${μ$_3$-AsFe(CO)$_4$}], ([Et$_4$N][VI]): To a solution of 1.0 g (1.2 mmol) of [Et$_4$N]$_2$[**I**] dissolved in 20 mL THF was added 0.31 g (1.2 mmol) $AgPF_6$ dissolved in 30 mL of THF over five minutes by cannula in the dark at room temperature. The resulting deep brown-orange solution was stirred in the dark for 30 minutes, and then filtered. The resulting solution was refluxed for three hours and then the solvent was removed *in vacuo*. To the residue were added 60 mL of diethyl ether. After three hours of stirring, the solution was filtered and stored in the fridge at -10 °C for two months. A few black crystals were recovered. Isolating enough pure material to submit for elemental analysis proved too difficult. ν_{CO} (DCM): 2071 (w), 2048 (w), 2032 (s), 2020. (s), 2002 (vs), 1968 (m, sh), 1955 (m), 1936 (m, sh) cm^{-1}. ^{1}H NMR data of crude solids (d_6-acetone, ppm) -20.693 (2H, s, broad); [Et$_4$N]$^+$ signals observed at 3.440 (8H) and 1.367 (12H) ppm. ESI-MS for crude solids prior to ether extraction *m*/*z* (%) 793.5 (51) [[Et$_4$N][**VI**]]$^-$ - H$^+$.

Synthesis of [Et$_4$N][(μ$_4$-As){FeMn(CO)$_8$}{Fe$_2$(CO)$_6$(μ-CO)(μ-H)}], ([Et$_4$N][VII]): To a mixture of 0.9 g (1.1 mmol) of [Et$_4$N]$_2$[**I**] and 0.3 g Mn(CO)$_5$Br (1.0 mmol) was added 30 mL of THF and the resulting deep-red orange solution was allowed to stir for 24 h. The solution was then filtered to remove a white precipitate and brought to dryness *in vacuo*. The resulting solids were treated with 40 mL diethyl ether, allowed to stand for 3 h at room temperature, filtered, and stored at -10 °C. Red-black crystals of [**VII**]$^-$ appeared overnight. Repeated washings with ethyl ether were required to recover maximum product. Yield: 490 mg, 52%. ν_{CO} (THF) 2111 (vw), 2078 (w), 2035 (s), 2018 (vs), 1987 (m), 1965 (s), 1938 (w), 1921 (w), 1779 (w) cm^{-1}. Anal. Calcd for $Fe_3MnAsC_{23}O_{15}H_{21}N$: C, 32.55; H, 2.49; N, 1.65. Found: C, 32.01; H, 2.54; N 1.64. ^{1}H NMR data (d_3-acetonitrile, ppm): 3.158 (8H, *q*, *J* = 7.5 Hz), 1.218 (12H, *t*, *J* = 7.5 Hz), -8.750 (1H, *s*). ESI-MS of the crude product before ether extraction: *m*/*z* (%): 718.4 (9) [**VII**]$^-$, 690.4 (50) [**VII**]$^-$-CO, 662.4 (12) [**VII**]$^-$-2CO, 634.4 (17) [**VII**]$^-$-3CO, 550.4 (2) [**VII**]$^-$-6CO, 522.5 (2) [**VII**]$^-$ -7CO, 494.5 (2) [**VII**]$^-$-8CO. Slightly soluble in ethyl ether; soluble in THF, MeOH, acetone, dichloromethane.

Synthesis of [Et$_4$N][{Fe$_3$(CO)$_9$(μ-CO)}(μ$_3$-AsMn(CO)$_4$Br-*cis*}], [Et$_4$N][VIII]: To a mixture of 0.9 g (1.1 mmol) of [**I**][2] and 0.3 g Mn(CO)$_5$Br (1.1 mmol) was added 30 mL of THF and the resulting deep-red orange solution was allowed to stir for 24 h. To the resulting mixture was added 0.5 mL triethylamine (3.6 mmol). An additional 0.6 g of Mn(CO)$_5$Br (2 mmol) in 10 mL of THF was added rapidly and the resulting mixture was refluxed for three hours and allowed to cool to room temperature followed by filtration and removal of the solvent *in vacuo*. The resulting solids were treated with 40 mL diethyl ether, allowed to stand for 3 h at room temperature, filtered, and stored at -10 °C. Several black rectangular prismatic blocks of [**VIII**]$^-$ appeared overnight. Isolating enough pure material to submit for elemental analysis proved too difficult although the ESI-MS data supports a higher yield than given above. ν_{CO} (DCM) 2088 (w), 2054 (m), 2022 (vs), 2010. (s), 1998 (ssh), 1984 (msh), 1964 (msh), 1950 (wsh), 1862 (vw, br) cm^{-1}. ESI-MS data collected for crude product prior to ether treatment (%): 768.4 (6) [**VIII**]$^-$, 740.4 (11) [**VIII**]$^-$ - CO, 656.4 (4) [**VIII**]$^-$ - 3CO, and 628.5 (8) [**VIII**]$^-$-4 CO.

Synthesis of (μ-H)$_2$Fe$_3$(CO)$_9${μ$_3$-AsMn(CO)$_5$}, IX: To a mixture of 0.9 g (1.1 mmol) of [**I**]$^{2-}$ and 0.3 g Mn(CO)$_5$Br was added 30 mL of DCM and the resulting deep-red orange solution was allowed to stir for 24 h. The solvent was then removed *in vacuo*. The resulting solid was transferred to a mortar and pestle and homogenized with 0.3 g (1.0 mmol) [CPh$_3$][BF$_4$]. 15 mL of DCM was rapidly added with stirring. After one hour, the solvent was removed *in vacuo*. Treatment of the solids with 20 mL of *n*-hexane with subsequent filtration and storage at -10 °C yielded red crystals of **IX** suitable for X-ray diffraction in <2% yield. Isolating enough pure material to submit for elemental analysis proved too difficult although the ESI-MS data supports a higher yield than given above. ν_{CO} (DCM): 2127 (w), 2076 (m), 2048 (vs), 2015 (s), 1985 (m, br), 1971 (w, br), 1957 (vw, br) cm^{-1}. ^{1}H NMR data for toluene extract following DCM removal (d_6-acetone, ppm): -23.379 (2H, m). ESI-MS of a toluene extract of the crude following DCM removal (%): 768.4 (7) **IX**-H$_2$+Br$^-$, 740.4 (7) **IX** - CO - H$_2$+Br$^-$, 690.4 (5) **IX** -H$^+$, 662.4 (13) **IX** - H$^+$ - CO, 634.4 (16) **IX** - H$^+$ -2CO, 550.4 (1) **IX**-H$^+$ -5CO, 522.5 (4) **IX**$^-$H$^+$-8CO, 494.5 (1) **IX** -H$^+$-9CO.

Synthesis of {FeMn(CO)$_8$}(μ$_4$-As){Fe$_2$(CO)$_8$}, X: To a mixture of 2.0 g (2.4 mmol) of [Et$_4$N]$_2$[**I**] $^-$ and 0.7 g (2.4 mmol) Mn(CO)$_5$Br was added 40 mL of THF. The resulting solution was stirred for 24 hours, filtered, and brought down to dryness. The solids were taken up in 30 mL of DCM and a solution of 274 μL (3.1 mmol) of trifluoromethanesulfonic acid in 10 mL DCM was degassed and added by cannula over five minutes' time. The resulting solution was allowed to stir for 24 hours subsequent to which the solvent was removed *in vacuo*. Crude product was obtained by extraction of the product into 40 mL of toluene, filtration, and evaporation. A small amount of **IX** was separated by treatment of the toluene with 0.5 mL triethylamine (3.6 mmol) prior to evaporation. Crystals suitable for X-ray diffraction were obtained by extraction with ether from the original solids obtained from the reaction following DCM removal or from the crude toluene extract. In each case, the ether was allowed to stand for three hours at room temperature, filtered, and stored at -10 °C for two days. Yield: 1.32 g, 74% (based on As) ν_{CO} (DCM): 2114 (w), 2071 (s, sh), 2066 (s), 2040. (vs), 2015 (m), 1993 (m), 1951 (w), 1939 (w, sh) cm^{-1}. Soluble in toluene, acetone, THF, and DCM. Anal. Calcd. for $Fe_3MnAsC_{16}O_{16}$: C, 25.78; H, 0.00; N, 0.00. Found: C, 25.45; H, 0.73; N, <0.5. The presence of H is attributed to a minor impurity of [Et$_4$N]Br, most likely [Et$_4$N]Br as weak signals incorporating the Br$^-$ ion are observed in the ESI-MS. ESI-MS of crystalline material (%): 768.2 (21) **X**-2CO+Br$^-$, 740.3 (4) **X** -3CO +Br$^-$, 719.3 (4) **X**-CO+2H$^-$, 691.3 (9) **X**-2CO+2H$^-$, 663.4 (7) **X**-3CO+2H$^-$, 656.4 (2) **X** -6CO+Br$^-$, 635.4 (1) **X**-4CO+2H$^-$, 628.4 (3) **X**-7CO+Br$^-$, 579.4 (1) **X**-6CO+2H$^-$.

Synthesis of [Et$_4$N][Fe$_3$(CO)$_9$(μ-CO){μ$_3$-PFe(CO)$_4$}]: To a slurry of 2.18 g [Et$_4$N]$_2$[Fe$_4$(CO)$_{13}$] (2.57 mmol) in 20 mL of DCM was added over five minutes time a solution of 173 μL of PCl_3 (1.94 mmol) in 20 mL of DCM via cannula at room temperature with stirring. Following addition, the resulting mixture was stirred for two hours and filtered. 60 mL of degassed water was added to the DCM and the DCM removed *in vacuo*. The remaining aqueous solution containing byproduct halide salts was filtered off and the crude product dried *in vacuo*. This was then redissolved in 30 mL of THF, filtered, and brought down to dryness *in vacuo*. Yield: 1.20 g, 80% (based on P). Crystals suitable for single-crystal X-ray diffraction were obtained by treating the crude product with 30 mL of diethyl ether, allowing to stand for 3 h, and filtering. The resulting solution was concentrated *in vacuo* and allowed to stand at room temperature for two weeks over the course of which small, brown-red plate-like crystals grew along the walls of the flask. ν_{CO} (THF): 2028 (s), 2012 (vs), 2003 (vs), 1986 (msh), 1970 (m), 1963 (m), 1800. (w) cm^{-1}. Anal. Calcd. for $Fe_4PC_{22}O_{14}NH_{20}$: C, 34.02; H, 2.60; N, 1.80. Found (Crude Product): C, 34.35; H, 3.65, N, 1.85. ^{31}P NMR data (d_3-acetonitrile, ppm, shifts relative to H_3PO_4, SR = - 70.45): 395.08 (1P, *s*). ESI-MS of the solids prior to ether extraction (%): 646.4 (23) [Fe$_3$(CO)$_9$(μ-CO)(μ$_3$-PFe(CO)$_4$)]$^-$, 618.4 (11)[Fe$_3$(CO)$_9$(μ-CO)(μ$_3$-PFe(CO)$_4$]$^-$-CO, 590.5 (45) [Fe$_3$(CO)$_9$(μ-CO)(μ$_3$-PFe(CO)$_4$]$^-$-2CO, 562.5 (4) [Fe$_3$(CO)$_9$(μ-CO)(μ$_3$-PFe(CO)$_4$]$^-$-3CO, 506.5 (3) [Fe$_3$(CO)$_9$(μ-CO)(μ$_3$-PFe(CO)$_4$]$^-$-5CO.

Single-Crystal X-ray Diffraction Considerations:

Diffraction data were collected on a Rigaku SCX-Mini diffractometer (Mercury2 CCD) using graphite monochromated Mo-Kα radiation (λ = 0.71073 Å). Integration was performed with CrystalClear-SM Expert 2.0 and the data corrected for absorption using empirical methods.[80] All structures were solved by direct methods and refined on F^2 by full-matrix least squares using the SHELXTL software package.[81]All thermal ellipsoid plots were generated using the Diamond software package.[82]All non-hydrogen atoms were refined anisotropically. The hydrogen atoms bound to $[Et_4N]^+$ were given idealized positions. A summary of X-ray data collection and refinement parameters for the compounds is given in **Tables S1, S2, S3, and S4** A summary of selected bond lengths and angles for the reported compounds is given in **Tables S5-S11**.

ASSOCIATED CONTENT

The Supporting Information is available free of charge on the ACS Publications website at DOI: 10.1021/acs.organomet.xxxxxxx. NMR spectra are available in **Figure SF1-SF5.** Nominal ESI-MS data is given in the Appendix. A summary of X-ray data collection and refinement parameters for the compounds is given in **Tables S1-S4.** A summary of selected bond lengths and angles for the reported compounds is given in **Tables S5-S11**. Full crystallographic details including solution, refinement and disorder modeling procedures are documented in CIF format (CIF).

AUTHOR INFORMATION

Corresponding Author

* Email: whitmir@rice.edu

ACKNOWLEDGEMENTS

D.E.S. acknowledges the National Science Foundation for a Graduate Research Fellowship, Martin Alexander Lange for assisting with some of the preparations of $[Et_4N]_2[\mathbf{I}]$, and Michael W. Hull, Michael J. McClain, and Felix Berg for productive discussions. This material is based upon work supported by the National Science Foundation under Grant No. CHE-1411495. The authors declare no competing financial interests.

REFERENCES

(1) Whitmire, K. H.; Caudell, J. B. In *Encyclopedia of Inorganic and Bioinorganic Chemistry*; John Wiley & Sons, Ltd, 2011.

(2) Hall, J. W.; Membreno, N.; Wu, J.; Celio, H.; Jones, R. A.; Stevenson, K. J. *J. Am. Chem. Soc.* **2012**, *134*, 5532–5535.

(3) Silva, D. C. C.; Crosnier, O.; Ouvrard, G.; Greedan, J.; Safa-Sefat, A.; Nazar, L. F. *Electrochem. Solid-State Lett.* **2003**, *6*, A162.

(4) Boyanov, S.; Bernardi, J.; Gillot, F.; Dupont, L.; Womes, M.; Tarascon, J.-M.; Monconduit, L.; Doublet, M.-L. *ChemInform* **2006**, *37*, 3531-3538.

(5) Jiang, P.; Liu, Q.; Liang, Y.; Tian, J.; Asiri, A. M.; Sun, X. *Angew. Chem. Int. Ed.* **2014**, *53*, 12855–12859.

(6) Zhang, Z.; Lu, B.; Hao, J.; Yang, W.; Tang, J. *Chem. Commun.* **2014**, *50*, 11554–11557.

(7) Callejas, J. F.; McEnaney, J. M.; Read, C. G.; Crompton, J. C.; Biacchi, A. J.; Popczun, E. J.; Gordon, T. R.; Lewis, N. S.; Schaak, R. E. *ACS Nano* **2014**, *8*, 11101–11107.

(8) Yang, X.; Lu, A.-Y.; Zhu, Y.; Min, S.; Hedhili, M. N.; Han, Y.; Huang, K.-W.; Li, L.-J. *Nanoscale* **2015**, *7*, 10974–10981.

(9) Oyama, S. T. *J. Catal.* **2003**, *216* , 343–352.

(10) Huang, X.; Dong, Q.; Huang, H.; Yue, L.; Zhu, Z.; Dai, J. *J. Nanoparticle Res.* **2014**, *16*, 1–6.

(11) Cruz-Silva, E.; Cullen, D. A.; Gu, L.; Romo-Herrera, J. M.; Muñoz-Sandoval, E.; López-Urías, F.; Sumpter, B. G.; Meunier, V.; Charlier, J.-C.; Smith, D. J.; Terrones, H.; Terrones, M. *ACS Nano* **2008**, *2*, 441–448.

(12) Broddefalk, A.; James, P.; Liu, H.-P.; Kalska, B.; Andersson, Y.; Granberg, P.; Nordblad, P.; Häggström, L.; Eriksson, O. *Phys. Rev. B* **2000**, *61*, 413–421.

(13) Carenco, S.; Portehault, D.; Boissière, C.; Mézailles, N.; Sanchez, C. *Chem. Rev.* **2013**, *113*, 7981–8065.

(14) Brock, S. L.; Senevirathne, K. *J. Solid State Chem.* **2008**, *181*, 1552–1559.

(15) Chen, J.-H.; Tai, M.-F.; Chi, K.-M. *J. Mater. Chem.* **2004**, *14*, 296.

(16) Qian, C.; Kim, F.; Ma, L.; Tsui, F.; Yang, P.; Liu, J. *J. Am. Chem. Soc.* **2004**, *126*, 1195–1198.

(17) Henkes, A. E.; Schaak, R. E. *Chem. Mater.* **2007**, *19*, 4234–4242.

(18) Layan Savithra, G. H.; Muthuswamy, E.; Bowker, R. H.; Carrillo, B. A.; Bussell, M. E.; Brock, S. L. *Chem. Mater.* **2013**, *25*, 825–833.

(19) Gregg, K. A.; Perera, S. C.; Lawes, G.; Shinozaki, S.; Brock, S. L. *Chem. Mater.* **2006**, *18*, 879–886.

(20) Barry, B. M.; Gillan, E. G. *Chem. Mater.* **2009**, *21*, 4454–4461.

(21) Singh, N.; Khanna, P. K.; Joy, P. A. *J. Nanoparticle Res.* **2008**, *11*, 491–497.

(22) Zhang, H.; Ha, D.-H.; Hovden, R.; Kourkoutis, L. F.; Robinson, R. D. *Nano Lett.* **2011**, *11*, 188–197.

(23) Colson, A. C.; Chen, C.-W.; Morosan, E.; Whitmire, K. H. *Adv. Funct. Mater.* **2012**, *22* (9), 1850–1855.

(24) Colson, A. C.; Whitmire, K. H. *Organometallics* **2010**, *29*, 4611–4618.

(25) Colson, A. C.; Whitmire, K. H. *Chem. Mater.* **2011**, *23*, 3731–3739.

(26) Hunger, C.; Ojo, W.-S.; Bauer, S.; Xu, S.; Zabel, M.; Chaudret, B.; Lacroix, L.-M.; Scheer, M.; Nayral, C.; Delpech, F. *Chem. Commun.* **2013**, *49*, 11788–11790.

(27) Bauer, S.; Hunger, C.; Bodensteiner, M.; Ojo, W.-S.; Cros-Gagneux, A.; Chaudret, B.; Nayral, C.; Delpech, F.; Scheer, M. *Inorg. Chem.* **2014**, *53*, 11438–11446.

(28) Tegus, O.; Brück, E.; Buschow, K. H. J.; de Boer, F. R. *Nature* **2002**, *415*, 150–152.

(29) Bachman, R. E.; Miller, S. K.; Whitmire, K. H. *Inorg. Chem.* **1994**, *33*, 2075–2076.

(30) Ehrl, W.; Vahrenkamp, H. *Chem. Ber.* **1973**, *106*, 2556–2562.

(31) Ehrl, W.; Vahrenkamp, H. *Chem. Ber.* **1973**, *106*, 2563–2569.

(32) Collins, B. E.; Koide, Y.; Schauer, C. K.; White, P. S. *Inorg. Chem.* **1997**, *36* , 6172–6183.

(33) Langenbach, H.-J.; Vahrenkamp, H. *Chem. Ber.* **1980**, *113*, 2189–2199.

(34) Langenbach, H.-J.; Röttinger, E.; Vahrenkamp, H. *Chem. Ber.* **1980**, *113*, 42–54.

(35) Madach, T.; Vahrenkamp, H. *Z. Für Naturforschung Teil B* **1979**, *34b*, 1195–1198.

(36) Müller, R.; Vahrenkamp, H. *Chem. Ber.* **1977**, *110* , 3910–3919.

(37) Bachman, R. E.; Miller, S. K.; Whitmire, K. H. *Organometallics* **1995**, *14*, 796–803.

(38) Bachman, R. E.; Whitmire, K. H. *Inorg. Chem.* **1994**, *33*, 2527–2533.

(39) In *Inorganic Reactions and Methods*; Zuckerman, J. J., Hagen, A. P., Eds.; John Wiley & Sons, Inc., 1988; pp i – xxii.

(40) Gourdon, A.; Jeannin, Y. *J. Organomet. Chem.* **1986**, *304*, C1–C3.

(41) Whitmire, K. H.; Leigh, S. L.; Shieh, M.; Fabiano, M. D.; Rheingold, A. L. *New J. Chem.* **1988**, *12*, 397–404.
(42) Canè, M.; Iapalucci, M. C.; Longoni, G.; Demartin, F.; Grossi, L. *Mater. Chem. Phys.* **1991**, *29*, 395–404.
(43) Angelici, R. J. *Inorg. Chem.* **1964**, *3*, 1099–1102.
(44) Deck, W.; Schwarz, M.; Vahrenkamp, H. *Chem. Ber.* **1987**, *120* (9), 1515–1521.
(45) Iiskola, E.; Pakkanen, T. A.; Pakkanen, T.; Venäläinen, T. *Acta Chem. Scand. A* **1983**, *37*, 125–130.
(46) Böttcher, H.-C.; Hartung, H.; Krug, A.; Walther, B. *Polyhedron* **1994**, *13*, 2893–2897.
(47) Arif, A. M.; Cowley, A. H.; Pakulski, M.; Pearsall, M.-A.; Clegg, W.; Norman, N. C.; Orpen, A. G. *J. Chem. Soc. Dalton Trans.* **1988**, 2713–2721.
(48) Ebsworth, E. A. V.; Sheldrick, G. M. *Trans. Faraday Soc.* **1967**, *63*, 1071–1076.
(49) Stubenhofer, M.; Kuntz, C.; Bodensteiner, M.; Timoshkin, A. Y.; Scheer, M. *Organometallics* **2013**, *32*, 3521–3528.
(50) Cherng, J.-J.; Lai, Y.-W.; Liu, Y.-H.; Peng, S.-M.; Ueng, C.-H.; Shieh, M. *Inorg. Chem.* **2001**, *40*, 1206–1212.
(51) Herrmann, W. A.; Koumbouris, B.; Zahn, T.; Ziegler, M. L. *Angew. Chem. Int. Ed. Engl.* **1984**, *23*, 812–814.
(52) Hulley, E. B.; Bonanno, J. B.; Wolczanski, P. T.; Cundari, T. R.; Lobkovsky, E. B. *Inorg. Chem.* **2010**, *49*, 8524–8544.
(53) Guldner, K.; Johnson, B. F. G.; Lewis, J. *J. Organomet. Chem.* **1988**, *355* (1), 419–425.
(54) Luo, S.; Whitmire, K. H. *Inorg. Chem.* **1989**, *28*, 1424–1431.
(55) Lagrone, C. B.; Whitmire, K. H.; Churchill, M. R.; Fettinger, J. C. *Inorg. Chem.* **1986**, *25*, 2080–2085.
(56) Whitmire, K. H.; Shieh, M.; Cassidy, J. *Inorg. Chem.* **1989**, *28* (16), 3164–3170.
(57) Luo, S.; Whitmire, K. H. *J. Organomet. Chem.* **1989**, *376*, 297–310.
(58) Haynes, W. M. *CRC Handbook of Chemistry and Physics, 93rd Edition*; CRC Press, 2012.
(59) Eveland, J. R.; Saillard, J.-Y.; Whitmire, K. H. *Inorg. Chem.* **1997**, *36*, 330–334.
(60) Röttinger, E.; Vahrenkamp, H. *J. Chem. Res. Synop.* **1977**, 76.
(61) Jones, C.; Williams, T. C. *J. Organomet. Chem.* **2004**, *689*, 1648–1656.
(62) Song, L.-C.; Wang, J.-Y.; Gong, F.-H.; Cheng, J.; Hu, Q.-M. *J. Organomet. Chem.* **2004**, *689*, 930–935.
(63) Song, L.-C.; Hu, Q.-M.; Fan, H.-T.; Sun, B.-W.; Tang, M.-Y.; Chen, Y.; Sun, Y.; Sun, C.-X.; Wu, Q.-J. *Organometallics* **2000**, *19*, 3909–3915.
(64) Huttner, G.; Mohr, G.; Pritzlaff, B.; Seyerl, J. V.; Zsolnai, L. *Chem. Ber.* **1982**, *115*, 2044–2049.
(65) Song, L.-C.; Hu, Q.-M.; Fan, H.-T.; Tang, M.-Y.; Yang, Z.-Y.; Lu, G.-L. *Organometallics* **2002**, *21*, 2468–2472.
(66) Raubenheimer, H. G.; Gruker, G. J.; van A. Lombard, A. *J. Organomet. Chem.* **1987**, *323*, 385–395.
(67) Arif, A. M.; Cowley, A. H.; Pakulski, M. *J. Chem. Soc. Chem. Commun.* **1987**, 622.
(68) Anema, S. G.; Barris, G. C.; Mackay, K. M.; Nicholson, B. K. *J. Organomet. Chem.* **1988**, *350*, 207–215.
(69) Anema, S. G.; Mackay, K. M.; Nicholson, B. K. *Inorg. Chem.* **1989**, *28*, 3158–3164.
(70) Wei, W.; Zheng, T.; Zhao, J.; Zeng, G.; Shi, Z.; Zhu, L. *J. Organomet. Chem.* **2015**, *777*, 67–70.
(71) Melzer, D.; Weiss, E. *J. Organomet. Chem.* **1983**, *255*, 335–344.
(72) Arnold, L. J.; Mackay, K. M.; Nicholson, B. K. *J. Organomet. Chem.* **1990**, *387*, 197–207.
(73) Lindley, P. F.; Woodward, P. *J. Chem. Soc. Inorg. Phys. Theor.* **1967**, 382–392.
(74) Shi, Y.-C.; Fu, Q. *Z. Für Anorg. Allg. Chem.* **2013**, *639*, 1791–1794.
(75) Sandstrom, J. *Dynamic NMR Spectroscopy*; Academic Press: New York, 1982.
(76) Henderson, P.; Rossignoli, M.; Burns, R. C.; Scudder, M. L.; Craig, D. C. *J. Chem. Soc. Dalton Trans.* **1994**, 1641–1647.
(77) Kruck, T. *Angew. Chem.* **1966**, *78*, 500–500.
(78) Reimer, K. J.; Shaver, A.; Quick, M. H.; Angelici, R. J. In *Inorganic Syntheses*; Angelici, R. J., Ed.; John Wiley & Sons, Inc., 1990; pp 154–159.
(79) Whitmire, K.; Ross, J.; Cooper, C. B.; Shriver, D. F.; Bradley, J. S.; Cote, W. J.; Krusic, P. J. In *Inorganic Syntheses*; Jr, J. P. F., Ed.; John Wiley & Sons, Inc., 1982; pp 66–69.
(80) Sheldrick, G. M. *SADABS, A Software for Empirical Absorption Correction.*; University of Göttingen: Göttingen, 2002.
(81) Sheldrick, G. M. *SHELXTL*; Bruker AXS Inc.: Madison, 1997.
(82) Brandenburg, K. *DIAMOND*; Crystal Impact GbR: Bonn.

Insert Table of Contents artwork here